Journal of
Advanced Manufacturing Science and Technology
jamst@jamstjournal.com;jamst2020@126.com
www.jamstjournal.com

Ultrasonic vibration-assisted micro-milling: A comprehensive review

Sami ULLAH[a], Zhiqiang LIANG[a,b,c,*], Yuchao DU[a,*], Zhipeng SU[a], Cheng GUO[d], Zhen YIN[e], Haofei GUO[a, b], Yoomi KIM[a], Tianfeng ZHOU[a,b], Xibin WANG[a]

[a] *School of Mechanical Engineering, Beijing Institute of Technology, Beijing 100081, China*
[b] *Beijing Institute of Technology Chongqing Innovation Center, Chongqing 401120, China*
[c] *Beijing Institute of Technology, Zhengzhou Academy of Intelligent Technology, Zhengzhou 450000, China*
[d] *Shenzhen University, Shenzhen 518060, China*
[e] *Suzhou University of Science and Technology, Suzhou 215009, China*

Received 22 January 2024; revised 15 March 2024; accepted 28 March 2024; Available online 3 September 2024

Abstract: Mechanical micro-milling has become a prominent micromachining technique in recent years, and it has advanced high machining efficiency and precision. The advantages of versatility, utility, cost-effectiveness, and efficiency make it suitable for varied industries such as biomedicine, electronics, aerospace, and aviation. However, Conventional Micro-Milling (CMM) faces difficulties, particularly in dealing with difficult-to-cut materials. To solve the above problems, Ultrasonic Vibration-Assisted Micro-Milling (UVAMM) is proposed, which can efficiently address the challenges of machining difficult-to-cut materials. UVAMM is able to inhibit chip formation and reduce the intense friction between the flank surface of the tool and the machined surface. What's more, it can reduce cutting forces, cutting temperature, and residual stress on the workpiece surface. Finally, it leads to an enhancement in the finished surface quality of difficult-to-cut materials, maximizing the overall machining performance. This paper reviewed UVAMM processing, such as mathematical modeling, chip formation, burr formation, tool wear, cutting forces, cutting temperature, and surface morphology. Furthermore, the finite element simulation of UVAMM and the significance of Minimum Quantity Lubrication (MQL) in UVAMM are discussed. At the end, advantages of UVAMM for difficult-to-cut materials such as titanium alloys, steel alloys, nickel-based alloys, aluminum alloys, composites, brass, and optical glass are summarized.

Keywords: Ultrasonic vibration-assisted micro-milling (UVAMM); Mathematical modeling; Chip formation; Surface roughness; Minimum quantity lubrication (MQL), Difficult-to-cut materials

1. Introduction

The need for precision and micromachining technologies, which are used to create mechanical components with characteristics that are measured in microns, has been rapidly increasing in biomedicine, electronics, aerospace, and aviation industries [1-8], as presented in Fig. 1. With the increasing demands of these industries, conventional micromachining techniques cannot meet the requirements since they have reached their upper limit [9-11]. To address this deficiency, it is necessary to investigate and implement novel micromachining techniques capable of efficiently fabricating complex mechanical components at the micron scale [12]. Specially, it involves laser microfabrication [13-15], lithography, electroplating and shaping (LIGA) [16,17], deep UV lithography [18,19], electrical discharge machining [20-22], deep reactive ion etching [23,24], and mechanical micromachining techniques [25-29]. These methods have very high precision and minor tolerances, but there are still many problems, such as working time, cost, material compatibility, thermal deformation, and preprocessing. In order to achieve greater productivity, cost-effectiveness, and processing flexibility, we require novel surface processing technologies that use conventional cutting techniques [12]. Previous studies show that ultrasonic vibration-assisted cutting (UVAC) proved to be an innovative technique to promote processing performance and product quality [30-32]. UVAC is a cutting method that improves cutting efficiency by applying vibration to a tool or workpiece [33]. The main idea of UVAC is to separate the tool and workpiece repeatedly. UVAC was first used in the late 1950s [34]. Then, UVAC is now widely used in the precision manufacturing of various materials. UVAC produces thinner chips and reduces cutting forces, resulting in higher machining efficiency, longer tool life, better surface quality, and a more precise shape while reducing burr formation [30,34-37].

Ultrasonic vibration-assisted micro-milling (UVAMM) is an advanced machining method that involves introducing vibration into

* Corresponding author. *E-mail address:* liangzhiqiang@bit.edu.cn(Zhiqiang LIANG), dycfelix@163.com(Yuchao DU)
Peer review under responsibility of Editorial Committee of JAMST
DOI: 10.51393/j.jamst.2025009

the machining process [33]. According to previous researchers, it can be classified into various types according to the vibration direction, which can be either one-dimensional [38], two-dimensional [39], or three-dimensional [40]. Ultrasonic vibration can be applied to either the cutting tool or the plane of the workpiece in UVAMM [38]. It plays an important role in satisfying the increasing need for tiny components with complex 3D geometries. The size effect has an impact on the blunt radius of cutting tools, and it is no longer acceptable to ignore it, especially when working with difficult-to-cut materials [41]. UVAMM is considered a highly effective method for machining difficult-to-cut materials. So, it leads to a distinctive cutting action in comparison to equivalent machining [42]. What's more, the latest research has shown significant interest in UVAMM for difficult-to-cut materials, which is able to solve the challenges resulting from conventional micro-milling (CMM). So, the researchers have extensively studied UVAMM, investigating its application in difficult-to-cut materials [43]. Based on these benefits of UVAMM, many researches concerning further machining mechanism were conducted. For example, relationship between the ratio of minimum chip thickness to cutting-edge radius and many parameters, such as the plowing effect, effective rake angle, and specific cutting energy of the machined surface, has been noted. Furthermore, it can directly impact the cutting performance and reduce the impact of both the size effect and the plowing effect [44-46]. Consequently, it can enhance cutting efficiency by avoiding these negative impacts.

UVAMM has revealed significant developments in recent years and offered a lot of benefits compared to CMM. Many studies have investigated the impact of various processing parameters, such as frequency, amplitude, workpiece material, microstructure, and effective tool trajectories, on output parameters such as chip formations, burr formation, tool wear, milling forces, milling temperature, and surface roughness. For example, UVAMM has enhanced efficiency in chip breaking through the application of ultrasonic vibrations [47], resulting in a reduction in unwanted burr formation, which is a common issue in CMM [48,49]. It can result in producing smoother and more precise machined surfaces. In addition, UVAMM helps reduce tool wear while improving their service life and cost-effectiveness [50]. UVAMM outperforms CMM by employing ultrasonic vibrations to help with the cutting process, resulting in reduced cutting forces and the generation of heat. This method improves material removal accuracy while reducing cutting forces [51,52], reducing cutting temperature [53], and leading to the improvement of precision and operational effectiveness. As a result, it produced a smoother and more precise machined surface by reducing the surface roughness in comparison to CMM [36,54].

The primary objective of this article is to provide an in-depth review of the most recent developments in UVAMM. It encompasses various aspects such as UVAMM processing, which include mathematical modeling, chip formation, burr formation, tool wear, cutting forces, cutting temperature, and surface morphology; the finite element simulation of UVAMM; the significance of MQL in UVAMM; and applications of UVAMM for difficult-to-cut materials such as titanium alloys, steel alloys, nickel-based alloys, aluminum alloys, composites, brass, and optical glass. The main purpose is to integrate and explain the most recent knowledge and developments in the field of UVAMM.

2.Ultrasonic vibration-assisted micro-milling (UVAMM) processing

In UVAMM, high-frequency and low-amplitude vibration is applied to the microscopic tool or workpiece to improve the efficiency of material removal, particularly for difficult-to-cut materials. Compared with CMM, UVAMM even removes dislocations within the crystal structure of the material that hinder the material's ability to deform and make it harder. By reducing dislocations, the material strength reduces and it becomes easier to cut, which helps to break the chips more effectively, and ultimately, the friction and heat generation between the cutting tool and the workpiece reduce. In addition, vibration helps to remove chips from the milling zone and prevent their re-engagement, which results in a reduction in cutting forces, tool wear, and burr formation. As a result, the material undergoes a change in its physical properties and becomes softer or more pliable, allowing for smoother cutting and improved surface finishes [55,56]. However, the significance of thermal softening compared to dislocation activation depends on the material properties and machining parameters. UVAMM has emerged as a potential response to the increasing difficulties in achieving higher levels of precision and efficiency in production [57,58]. Fig. 2 illustrates different types of ultrasonic vibration-assisted milling (UVAM) and categorizes them based on distinct tool tip path characteristics. Every type presents distinct benefits and is appropriate for specific applications. Fig. 3 illustrates the percentage of studies conducted in UVAMM processing that involve different output parameters such as mathematical modeling, chip formation, burr for-

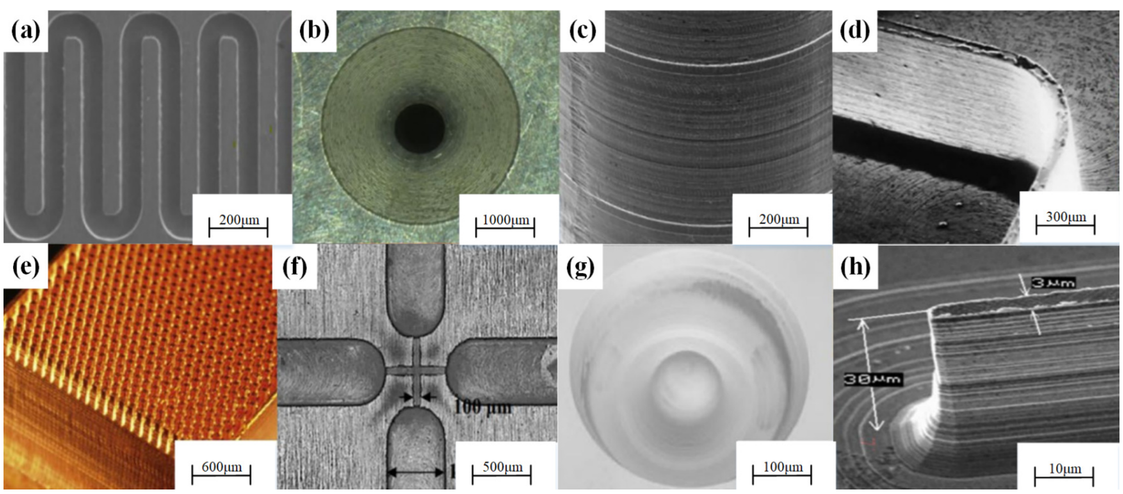

Fig. 1 High precision micro milling structures (a) Electric vacuum amplifier [1] (b) Micro-nozzles [2] (c, d) Micro-machining components [3,4] (e) Micro-pin fins [5] (f) Micro-channels [6] (g, h) Micro-molds [7,8]

mation, tool wear, cutting forces, cutting temperature, and surface morphology.

2.1. Mathematical modeling of machining mechanism

The introduction of mathematical modeling in UVAMM offers an organized approach to understand and improve the complex relationships inside machining processes. The researchers aim to represent the changing relationships between the different components which influence UVAMM by employing mathematical equations. This model can accurately assess the quantitative effects of ultrasonic vibration on variables such as tool wear, milling force, and surface quality [50,59,60]. By employing mathematical models, researchers can simulate and predict the complex movement of tools and workpieces in the context of UVAMM [50,61]. This enables them to gain significant insights into optimizing the process, developing tools, and enhancing overall performance in micro milling applications. Table 1 provides an overview of the mathematical models that have been developed using UVAMM.

2.2. Chip formation

Undeformed chip thickness is an important consideration in micro-milling as it directly impacts chip formation, milling forces, surface roughness, and tool wear. The significance of it resides in its size, which is comparable to the radius of the cutting edge, leading to possible scale effects. Consequently, numerous models have been suggested for predicting the undeformed chip thickness in micro-milling [63]. However, the chip thickness produced in UVAMM different from that in CMM because of the alteration in the tool tip's relative path. The difference becomes more evident when the design of the object that is being worked on develops complex and experiences vibration [49].

In the field of micromachining, the impact of the cutting-edge radius becomes noticeable when the thickness of the chip that has not been deformed falls below a specific value known as the minimum chip thickness, as presented in Fig. 4. The minimum chip thickness has a major impact on several machining factors, including as milling forces, tool wear, surface integrity, and process stability. Hence, it is essential to determine the minimum chip thickness in order to choose suitable machining conditions [64].

The microchip removal method illustrated in Fig. 5 demonstrates the essential importance of the minimum chip thickness. When the undeformed chip thickness (h) is below the minimum chip thickness (h_{min}) [65], as illustrated in Fig. 5(a), the cutting tool only applies force to the material without generating chips. This results in elastic deformation and affects the surface quality. As h reaches h_{min} in Fig. 5(b), chips start to form due to the shearing activity in the main shear zone, and the impact of ploughing becomes noticeable. When h is more than h_{min} (as seen in Fig. 5(c)), there is a continual generation of chips due to stable plastic deformation in the shear zone, even though there is some elastic material recovery. Usually, the initial thickness of the chip (h) is greater than the amount of material being removed, comparable to the way material is removed in quasi-homogeneous materials [63]. Son et al. [66] presented an advanced approach for ultra-precision cutting. The purpose of the model is to calculate the smallest possible thickness of an unaltered metal chip, known as the minimum chip thickness (h_{min}).

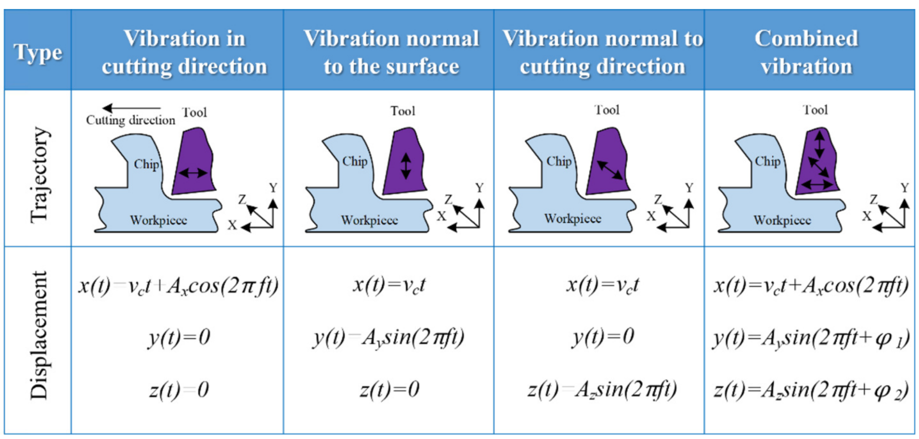

Fig. 2 Types of ultrasonic vibrations in milling process.[62]

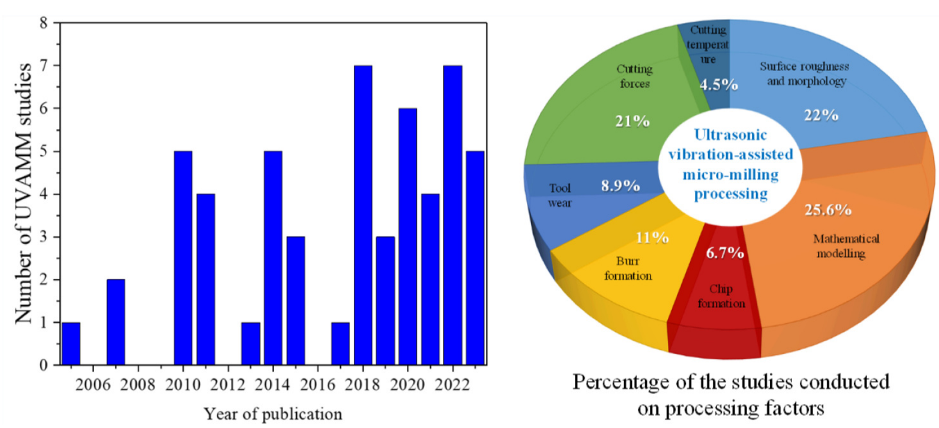

Fig. 3 Development trend of the UVAMM studies.

$$h_{\min} = \frac{r_e}{\left(1-\cos\left(\frac{\pi}{4}-\frac{\beta}{2}\right)\right)} \tag{1}$$

In Eq. (1), $h_{\min}$ is minimum undeformed chip thickness, r_e is radius of the blunt circle of the cutting edge, and β is the friction angle between the tool and the workpiece material.

On the other hand, a phase difference between two adjacent tool cutting trajectories during UVAMM machining will cause a change in the chip thickness. Some sections of the chip observe a relative increase in thickness, while other sections maintain a relative thin-

Table 1 Summary of mathematical modeling in UVAMM.

No.	Authors	Year	Vibration type	Mathematical models
1	Ding et al. [49,59]	2010-2011	2D	Machining process dynamics, milling force model, tool kinematics trajectory, chip thickness model
2	Lian et al. [37]	2013	1D	Tool kinematics trajectory
3	Ibrahim et al. [38]	2014	1D	Cutting tolerance, surface finish, tool wear
4	Ibrahim et al. [70]	2015	2D	Kinematic motion trajectory of tool
5	Chen et al. [71]	2018	2D	Dynamic analysis of vibrator, tool kinematic trajectory, surface texture generation
6	Zheng et al. [72]	2019	1D, 2D	Surface generation modeling
7	Zhang et al. [73]	2019	1D	Cutting force prediction model, undeformed chip thickness model
8	Mokhtari et al. [39]	2019	2D	UVAMM system model, motion model
9	Tan et al. [54]	2019	2D	Principle of UVAMM
10	He et al. [74]	2019	1D	Mechanism of UEVAMM
11	Sobamowo et al. [75]	2020	1D	Cutting force model, dynamic behavior, chip thickness
12	Zheng et al. [50]	2020	2D	Tool kinematic trajectory, tool-workpiece separation
13	Shang et al. [61]	2020	2D	Tool kinematic trajectory, tool-workpiece separation
14	Huan et al. [53]	2022	2D	Tool kinematic trajectory
15	Yuan et al. [76]	2022	1D	Tool kinematic trajectory
16	Shang et al. [77]	2022	2D	Cutting temperature model
17	Yuan et al. [78]	2022	1D	Tool kinematic trajectory
18	Yan et al. [40]	2023	2D	Surface formation mechanism
19	Zhang et al. [48]	2023	1D	Tool kinematic trajectory
20	Su et al. [79]	2023	3D	Tool kinematic trajectory, surface topography model

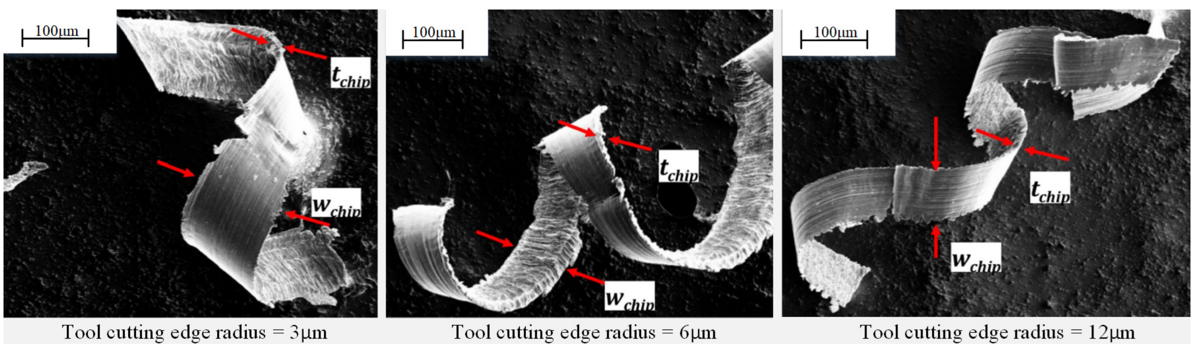

Fig. 4 Effect of micro milling tool cutting edge radius on chip morphology.[41]

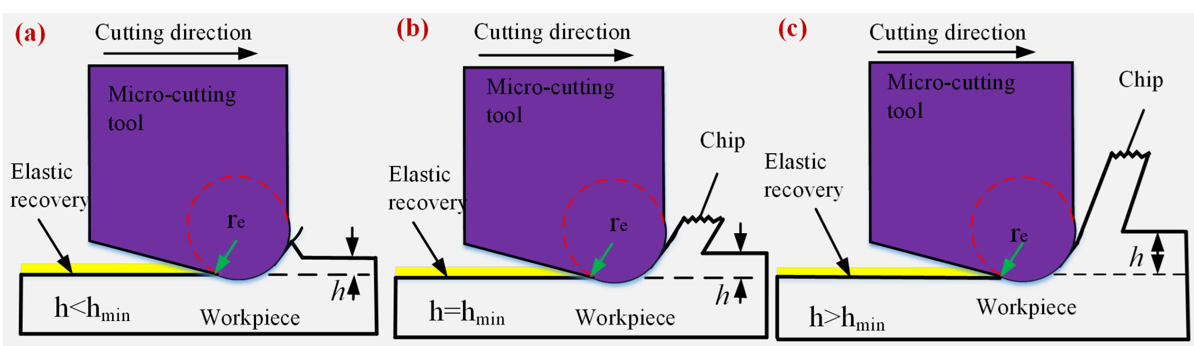

Fig. 5 Illustration of microchip removal mechanism.[80,81]

ness. Therefore, these elements have a natural tendency to break. The chips generated under these circumstances exhibit significant differences in terms of thickness and length when compared to those produced in a CMM. The phenomenon demonstrates the unique thickening cutting properties that are specific to the UVAMM process. According to Fig. 6(a), chip production in UVAMM mostly involves the extrusion process occurring between the cutting edge and the workpiece. Moreover, chip creation in UVAMM involves a combination of expansion and edge impact. Chip deformation is caused by the application of ultrasonic stress. It is important to mention that in UVAMM, although the undeformed cutting thickness (h) being smaller than the minimum cutting thickness (h_{min}) needed for conventional chip production, ultrasonic vibration can increase the cutting thickness over h_{min}, resulting in periodic modifications in the cutting shape. Fig. 6(b) demonstrates the effectiveness of ultrasonic vibration in continuously maintaining the cutting thickness at a steady value [48,78]. In addition, once the cutting-edge radius and material are determined, the minimum cutting thickness in UVAMM becomes a constant value. For a given cutting edge radius and material, such as Inconel718, the minimum cutting thickness remains constant, irrespective of other variables. Eq. (2) is a mathematical formula for determining the minimum chip thickness for cutting Inconel718 [82].

$$h_{min} = 0.25 \tag{2}$$

where, r_e represent the cutting-edge radius.

Fig. 7(a) illustrates the shear deformation that takes place in the chips while conventionally cutting a ductile material. The main shear deformation takes place within the shear plane, whereas the secondary shear deformation is a result of the friction between the chip and the tool. In conventional cutting, the deformation zone resulting from secondary friction is oriented in the opposite direction of the chip flow. This leads to the production of a shear flow shape, as illustrated in the figure. The shear flow is influenced by the elliptical trajectory of the cutting tool and the reversal of the frictional direction. The shear angle (ϕ_{EVC}) in ultrasonic elliptical vibration cutting (UEVC) is typically greater than in conventional cutting because of the elliptical tool path. Fig. 7(b) demonstrates that a greater shear angle leads to a decrease in chip thickness, which in turn leads to a decrease in milling force. UEVC is a cutting technique where the cutting process occurs in an elliptical path within a plane that includes the cutting and chip flow directions, as illustrated in Fig. 8. In the case of brittle materials (as shown in Fig. 8(a)), the UEVC technique utilizes a greater tool amplitude in the thrust direction, leading to a larger uncut chip thickness (t_{uc}) compared to typical cutting. The UEVC method applied to ductile materials (as shown in Fig. 8(b)) results in the formation of smooth and continuous chips due to the workpiece material's ability to deform without breaking. While the overall shape of the chip seems comparable in Fig. 7(a) and 8(b), there is a variation in the shear flow within the chip. UVAC of materials that can bend without breaking, friction between the material and the tool causes a distortion in the shear flow lines along the elliptical direction of the tool, compared to the direction of cutting [83].

The determination of chip thickness parameters in UVAMM is influenced by two primary criteria [67-69]: 1) The free time ratio (FTR) refers to the period in which the tool is not actively removing material in cutting mode. The measurement of the cut area is of utmost importance, and the proportion of time during which cutting does not occur is referred to as the *FTR* in 2-D UVAMM. It can be expressed in writing form.

$$\mathrm{FTR} = \frac{T_{\mathrm{nocutting}}}{T_{\mathrm{validtime}}} \times 100\% \tag{3}$$

$T_{nocutting}$ refers to the duration during which the tool tip is present in the cutting region without cutting, whereas $T_{validtime}$ indicates the overall duration during which the tool tip is present in the cutting area. FTR is influenced by the vibration and cutting conditions. Enhancing FTR by the optimization of vibration and cutting settings leads to improved chip evacuation conditions, enhanced cutting accuracy, and improved tool life [34]. 2) The amplitude ratio (AR) addresses the issue of variations in the distribution of chip thickness in 2-D UVAMM, particularly noticeable during micro milling. AR analysis is utilized to calculate the extent of these variations, which is technically defined as

$$\mathrm{AR} = \frac{A_{\mathrm{vibration}}}{f_z} \times 100\% \tag{4}$$

The term $A_{vibration}$ refers to the maximum magnitude of the chip thickness, while f_z represents the feed per tooth. Minor tool-workpiece collisions influence material removal, but greater *AR* values result in more significant collisions. When collisions exceed critical levels, they might cause damage to the tools. This emphasizes the important function of AR as a factor that reflects and influences the 2-D VAMM process.

Several researchers conducted a study on the chip formation mechanism in UVAMM, providing valuable insights and methodologies. Zhang et al. [73] developed a technique to measure tool vibration in real-time by employing differential equations of motion. This method enables the addition of process damping effects as feedback to control the undeformed chip thickness. Yuan et al. [78] investigated the impact of cutting conditions on chip formation in UVAMM and made a comparison with CMM. Their findings demonstrated that without ultrasonic vibration, chips of considerable

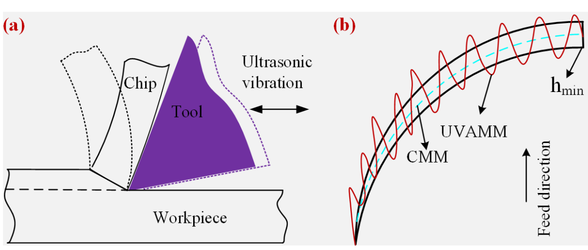

Fig. 6 Illustration of Chip formation process in UVAMM (a) Effect of chip deformation (b) Increases *h* in cutting.

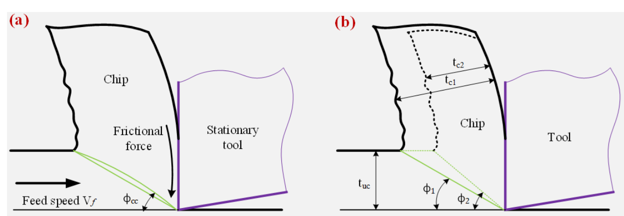

Fig. 7 Chip formation mechanism[83] (a) Ductile material in conventional cutting (b) Effect of the shear angle on the chip thickness.

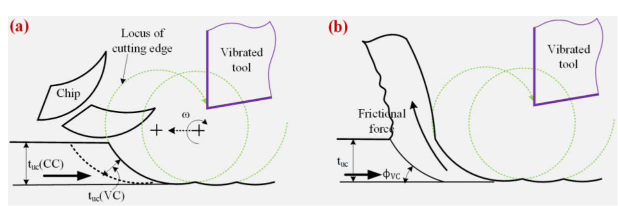

Fig. 8 Illustration of chip formation mechanism in elliptical vibration cutting[83] (a) brittle material (b) ductile material.

length and spiral shape were generated. However, the application of ultrasonic vibration causes a conversion of spiral chips into C-shaped chips, an improvement that becomes particularly evident when the amplitude to feed ratio (A/f_z) exceeds 1/2. This observation suggests a transition from a continuous cutting phase to an alternating cutting mode. In a study conducted by Li et al. [84] chip morphology was compared between CMM and UVAMM by experimental methods. Their investigation focused on the form of chip breakage and its effect on the bottom of the groove. The findings indicated that vibration had an important effect on the chip's morphology, resulting in variations in wrinkle height across several regions, as shown in Fig. 9(a). This phenomenon is caused by the constant variation of the undeformed cutting thickness during the cutting process, leading to periodic variations in the shape of the chip. Chen et al. [85] studied the effect of various vibration frequencies on the chip breaking mechanism of UVAMM. According to their research findings, continuous chips were created without any obvious cracks when there was no vibration present. However, raising the frequency of elliptical vibration from 6 kHz to 30 kHz results in a change in the location where cracks start, moving from the vicinity of the cutting edge to the area of shear and ultimately upwards. Furthermore, cracks become more prominent causing the chips more susceptible to cracking and ultimately resulting in the formation of irregular chips, as shown in Fig. 9(b).

Kiswanto et al. [47] specifically studied the modeling of chip shape in the context of 2D UVAMM. They constructed a theoretical model of the chip's shape using MATLAB, considering the position of the cutting tool's edge both before and after the application of ultrasonic vibration in the X-Y dimension. In addition, the model has a variable known as the bottom cutting edge angle that accurately represents the features of the cutting edge. Kim and Loh[83] investigated the microscopic features of chip generation in V-shaped groove with the use of elliptical vibration. The researchers conducted a comparison between the findings obtained via CMM and UEVAMM. They observed that CMM yielded chips with greater thickness and a wider radius of curvature compared to those made by UEVAMM. UEVAMM is anticipated to generate continuous chips since the depth of cut exceeds the magnitude of the elliptical tool path. However, the expansion of chip curvature is restricted. This phenomenon is caused by the counter-directional secondary friction in the shear deformation zone and the rise in shear angle, which functions as a chip breaker and results in the creation of discontinuous chips. Studies suggest that as the friction between the cutting tool and the chip reduces, the shear angle increases and the chip thickness reduces.

The investigations on UVAMM chip formation provide useful insights into the complex relationship between cutting parameters, vibration characteristics, and material properties. Through comprehension of these relationships, we may enhance the UVAMM process to optimize chip control, surface finish, and overall machining performance.

2.3. Burr formation

Burr formation is like chip formation and is a common phenomenon in the machining process. Fig. 10 shows that it is a significant factor when evaluating machined surfaces. Burrs are formed through the plastic deformation of the material towards the completion of the cutting process. Various factors influence the production of burrs, such as cutting parameters, tool geometry, workpiece geometry, manufacturing process, and material properties [41,78] as illustrated in Fig. 11. Burrs have a negative effect on the life of the product and the precision of the processing. Therefore, further deburring or edge finishing techniques are frequently necessary, however these methods can be expensive and ineffective. Furthermore, the deburring procedure has the potential to produce unnecessary residual tension and potentially cause damage on the component. Moreover, the deburring procedure becomes more complex for micro components due to their smaller size, and these parts are very prone to damage during machining, resulting in their removal as waste.

The first investigations on the phenomenon of burr development during machining processes can be tracked back to the 1970s [86]. These experiments demonstrate that the metal cutting area experi-

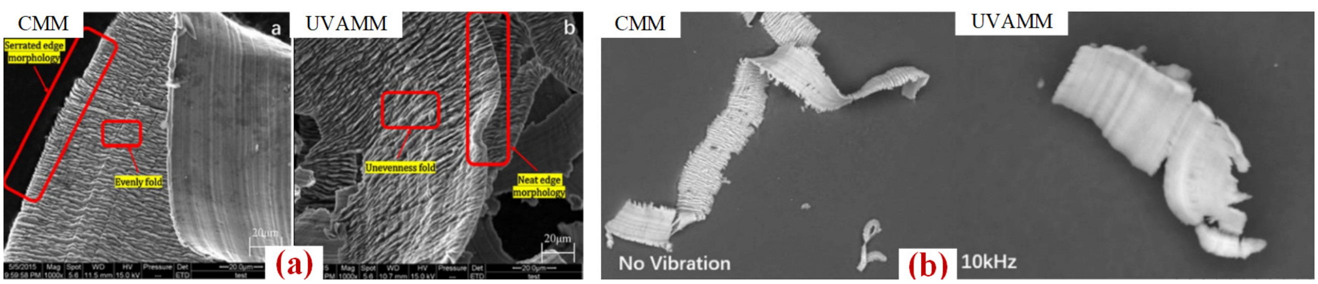

Fig. 9 Chip breaking in UVAMM (a) Li et al. [84] (b) Chen et al. [85]

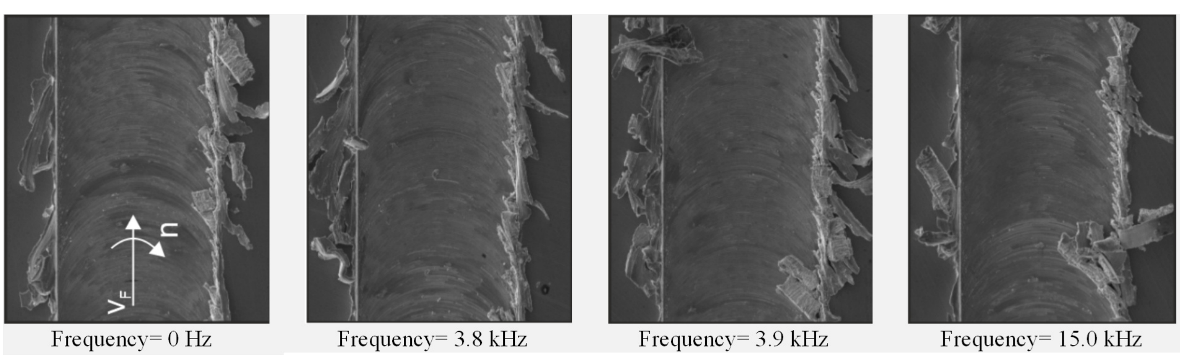

Fig. 10 Top burr on the micro milled surface in brass (CuZn39Pb2) with and without vibration from 0-15kHz frequency.[52]

ences substantial shear deformation when subjected to the tool's action, leading to notable shear forces and plastic deformation during the cutting process. Burrs are formed because of residual material remaining on the workpiece during the cutting process. Regarding burr production, the processing of burrs can be categorized into four types: rollover burr, tear burr, cut-off burr and Poisson burr, as illustrated in Fig. 12. Rollover burr: These burrs referred to as exit burrs, are conical shape that typically develop at the last stage of the machining procedure. Tear burr: These burrs result from the material tearing from the workpiece, rather than being removed by shearing. They are comparable to the burrs that form during the stamping process. Cut-off burr: These burrs formed from the early separation of the workpiece from the raw material before the completion of the cutting process. Poisson burr: These burrs develop due to the material's tendency to expand horizontally when subjected to compression, leading to irreversible plastic deformation.

In another approach burrs can be categorized according to their shape, position, and formation method. These categories include entry burrs, exit burrs, side burrs, and top burrs [89] as illustrated in Fig. 13. The four types of burrs show differences in both size and the mechanisms by which they are formed. The top burrs, which are generated by Poisson burrs and tear burrs, can be found on the upper surface of the workpiece. After the milling operation is completed, exit burrs adhere to the machined edge, whereas side burrs adhere to the newly formed surface [90].

The edge radius or edge radius ratio of the cutting tool plays an important role in micromachining. In contrast to conventional machining, where the edge radius may be ignored but the edge radius plays a key role in micromachining and has a notable impact on the cutting process [92]. As illustrated in Fig. 14, at high cutting speed (v_w), the cutting layer approaching the cutting-edge results in the generation of chips along the shear sliding surface OD by compression and shear deformation. However, the impact of the effective rake angle ($-\gamma_n$) on chip formation and burr formation is more significant than that of the nominal rake angle (γ_0), due to the existence of the cutting-edge radius (r_e). The material is unable to travel along the OD plane within the cutting-edge radius. Instead, it is pushed out by the *AB* area, resulting in the formation of the ma-

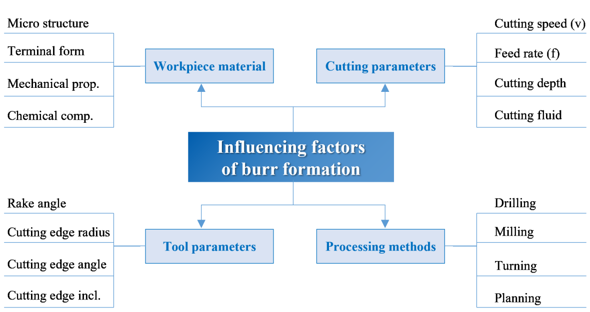

Fig. 11 Factors Influencing on burr formation.[78]

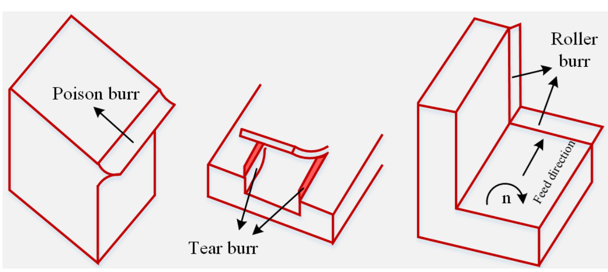

Fig. 12 Illustration of Poisson burr, tear burr and rollover burr.[87,88]

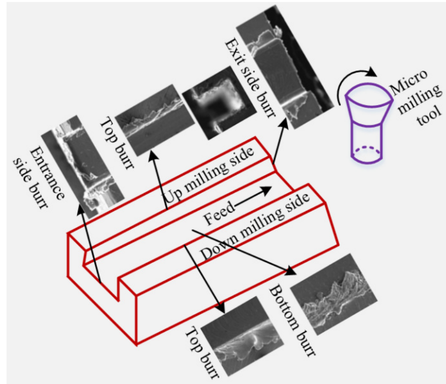

Fig. 13 Types of burrs in micro end milling.[86,87,91]

chined surface. The Δh layer indicates the height at which elastic recovery occurs. As the cutting tool approaches the edge of the workpiece, plastic deformation occurs, resulting in a negative shear zone. This causes part of the workpiece to shift because it lacks support from the surrounding material. The negative shear zone is subsequently connected to the positive shear zone. Burrs in plastic metals primarily develop due to the plowing force exerted following the removal of chips [93,94].

One interesting finding from this analysis is that burrs mainly form close to the outer edges or surfaces of the workpiece material because of the negative shear zone. To avoid the creation of burrs, it is crucial to minimize negative shear zones, particularly near the edges of the workpiece. An innovative strategy to address the difficulty of reducing the cutting-edge radius is to utilize support materials to strengthen the boundaries of the workpiece. Fig. 15 demonstrates that the process of placing support material onto the workpiece and enveloping it in a thin layer is an excellent method for transferring burrs from the workpiece to the support material. By eliminating the support material, it is possible to achieve a surface that is free of burrs, while still preserving the original geometry of the workpiece, such as maintaining perfect angles at the edges [93].

Fang et al. [82] proposed a formula to calculate the burr height in micro milling.

$$B_w = \frac{1}{n}\sum_{i=1}^{n}\Delta w_i \tag{5}$$

where n represent the number of positions, B_w is the average value of burr width and w_i is burr width of the ith point.

The researchers investigated the reduction in burr formation in

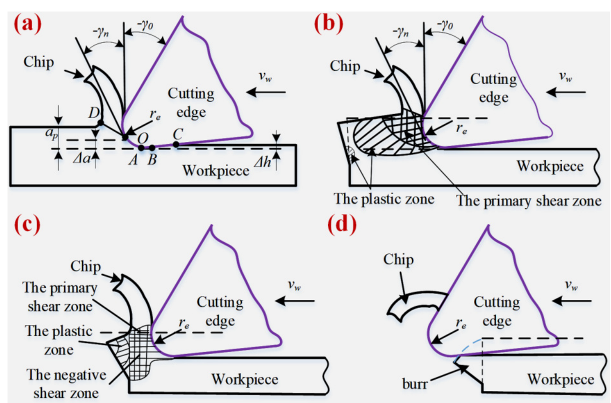

Fig. 14 Burrs formation mechanism in micro milling.[93] (a) The effect of ratio of edge radius to depth-of-cut on burr formation. (b) Initiation of burr formation. (c) Development of burr formation. (d) Final formation of burr.

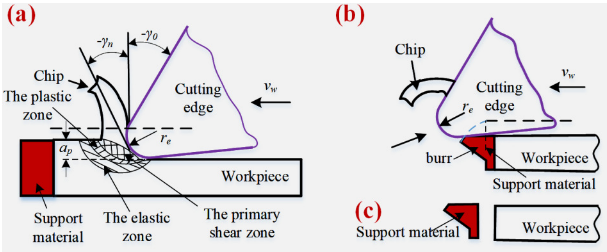

Fig. 15 Burrs prevention mechanism in micro milling. (a) Pretreatment with support material. (b) Burr existence in support material. (c) Removal of support material. [93]

UVAMM in comparison to CMM. Kim and Loh[83] conducted a study on the micro-V-shaped groove processing of copper. They used a cutting depth of 20μm and a cutting speed of 5 mm/s. The researchers also investigated the formation mechanism of exit burrs. They noted that UEVC did not cause exit burrs, whereas CMM micro-V-grooving resulted in exit burrs due to the cutting tool moving away from the workpiece. Chen et al. [35] investigated the method by which UVAMM reduces errors. The researchers conducted kinematic analysis and finite element modeling of microgroove milling. It was discovered that the tool consistently moved up and down the side of the groove because of the vibrations that helped it move in the feeding direction. This minimizes the burr formation. Both simulation and experimental data validate that the presence of vibrations during the micro milling process leads to a significant reduction in top burrs on the down-milled side of the slot, in comparison to the CMM. Li et al. [95] investigated the impact of vibration parameters on the formation of exit burrs. It was observed that the size of the exit burr increased as the diameter expanded from 18 mm to 25 mm, and as the vibration frequency increased from 2 kHz to 4 kHz. This occurs due to an enhancement of vibration frequency within the 2-4 kHz range, resulting in a more prominent plowing impact on the surface of the workpiece. This effect is accompanied by the creation of secondary cutting edges. Additionally, this alters the form of the chips generated during the process of machining. At a vibration frequency of 10 kHz, the size of the exit burr reduces to 3mm. Increased vibration frequency leads to a higher cutting speed, exceeding the rate at which the workpiece deforms. This results in improved chip breaking and a decrease in the production of burrs. As the vibration amplitude increases from 1 mm to 4 mm, the size of the exit burr reduces from 22 mm to 2 mm. Li and Wang [36] performed slot micro-milling experiments using up-milling technique with complete immersion and vibration. It was discovered that burrs developed on one side of the machined surface, whereas down-milling burrs formed on the opposite side. The production of burrs is not considerably influenced by the rate at which the material is fed. The burrs produced during up milling are extremely small, similar in size to UVAMM and CMM. The presence of mounting burrs was slightly reduced across all feed rates in the UVAMM system. After completing the cutting experiments with a cutting length of 168 mm, the up-milling burrs in UVAMM were found to be reduced by 16.0%, 17.5%, and 18.6% compared to CMM. Ding et al. [49] investigated the impact of size on the formation of top burr in 2D UVAMM. It was discovered that the amount of feed per tooth greatly impacts the height of the top burr. Additionally, employing vibration-assisted cutting in micro-end milling can reduce the size effect and enhance cutting efficiency, resulting in a reduction in the height of the top burr. Furthermore, the careful selection of suitable vibration parameters can significantly reduce the height of the upper burrs. Fang and Zhang [48,78] conducted a study on the mechanism of burr formation in CMM and UVAMM. They used simulation techniques to investigate this process and then validated their findings through comparable experiments. It was discovered that employing high-frequency ultrasonic vibration in the direction of milling feed can decrease cutting temperature and cutting force, enhance chip breaking capability, and reduce burr formation. Han et al. [96] evaluated the impact of horizontal ultrasonic vibration on the formation of burrs in UVAMM. Their investigations shown that horizontal vibrations can change the burr shape from a larger cluster to a unified sheet-like structure that rests on micro-grooves. Enhancing the magnitude of vibration reduces the rise of the side burrs and breaks them into small pieces. Furthermore, the implementation of horizontal vibration has the advantageous effect of reducing the length of burrs in micro-milling grooves, particularly when the feed rate exceeds the minimum cutting thickness by a little range. He et al. [74] conducted a comparison between UVAMM and EUMM, which involves the use of electric fields to induce ultrasonic vibrations during micro milling. Both procedures assist in the removal of burrs during the process of machining. It is important to mention that EUMM does not exhibit significant burr formation on both sides of the microchannel, resulting in a significant enhancement in processing quality. The average burr length at a rotational speed of 60,000 rpm for EUMM is just 15 µm, in comparison with 58 µm for UVAMM and 361 µm for CMM.

2.4. Tool wear

During machining, the cutting tool and the workpiece experience significant friction because of direct metal-to-metal contact. The friction generated at tool contact surfaces results in significant stress and heat, ultimately causing inevitable tool wear. Damaged tools will have a negative impact on the precision of machining and the quality of the surface, leading to a decrease in cutting effectiveness and an increase in machining costs [97,98]. Optimizing the service life of tools and maintaining the quality of products are important for establishing efficient and effective machining operations. Optimizing cutting parameters is a widely used technique to reduce tool wear and improve the tool life [99-101]. However, the efficiency of this method has limitations by conventional machining. Vibration-assisted machining provides an achievable solution for minimizing tool wear. By adding vibration into the machining process, both the tool and workpiece undergo regular cycles of separation and contact, resulting in a decrease in total friction and wear [102,103]. Fig. 16 shows the application of vibration can reduce tool wear in micro milling.

Tool wear can be classified into two different types: abnormal wear and normal wear, as graphically illustrated in Fig. 17. Abnormal wear typically occurs due to impact or uneven heating during processing, leading to brittle damage such as chipping, cracking, spalling, or deformation. Normal wear is a steady phenomenon

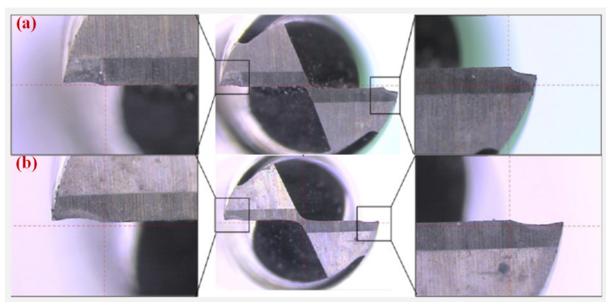

Fig. 16 Tool wear [104] (a) CMM (b) UVAMM.

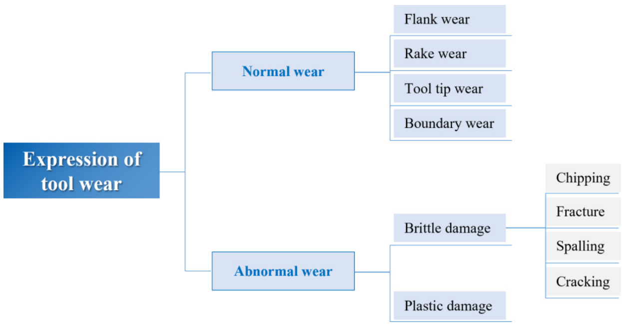

Fig. 17 Classification of tool wear.

characterized by the gradual degradation of tools as time passes. The phenomenon of rake tool wear, flank wear, tool tip wear, and boundary wear during machining can be due to friction and temperatures. [105].

UVAMM has significant advantages in improving tool life. The efficiency of reducing tool wear is dependent upon the precise cutting process, which is influenced by varying tool-workpiece separation conditions. Zheng et al. [50] proposed that UVAMM has the capability to establish three distinct and continuous states of separation between the tool and the workpiece. These conditions are illustrated in Fig. 18. To establish the initial separation between the tool and workpiece, the vibration velocity of either the tool or workpiece (V_v) must exceed the nominal cutting speed (V_n). The term "nominal cutting speed" refers to the pace at which the tool tip moves without any assistance from vibrations. The standard can be expressed in this way:

$$\left[V_v = 2\pi f_x A_x \cos\left(2\pi f_x t+\varphi_x\right)\cos\alpha\right] \geqslant \left[V_n = \frac{\pi r n}{30}\right] \tag{6}$$

$$\cos\left(2\pi f_x t+\varphi_x\right)\cos\alpha \geqslant \frac{rn}{60 f_x A_x} \tag{7}$$

Eq. (7) is only valid when

$$\frac{rn}{60 f_x A_x} \leqslant 1 \tag{8}$$

In the above equations, f_x and A_x represent the vibration frequency and amplitude, respectively, whereas φ_x is the initial vibration phase angle.

A comprehensive investigation has been conducted on the phenomenon of tool wear in CMM. Wang et al. [106] and Dawodinejad et al. [107] conducted thorough research on tool wear in micro-milling, specifically investigating its impact on surface roughness and chip formation. However, only a limited number of research have investigated its behavior with the assistance of ultrasonic vibrations. Greco et al. [51] conducted a comparison between UVAMM and CMM and observed that whereas CMM tools exhibited noticeable wear on the main cutting edges and corners, vibration reduced this wear, as shown in Fig. 19(a). The absence of built-up edge formation and tearing during UVAMM is the cause of this decrease in wear. Fang and Yuan [82,108] conducted an analysis of tool wear in UVAMM and discovered that vibration decreased the occurrence of built-up edge development on the rake face of the cutting tool, as shown in Fig. 19(b).

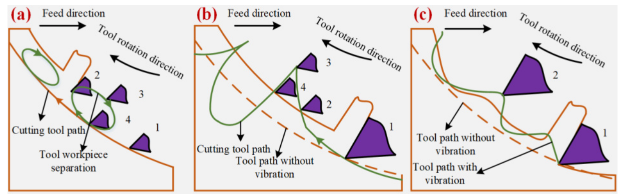

Fig. 18 Three types of tool workpiece separation conditions.[50]

Chern et al. [34] observed that employing vibration assistance in micro milling can enhance the production of grooves within the acceptable tolerance range. Without any vibration, the tool's life is limited to just 80 grooves. However, when subjected to an ultrasonic frequency of 500 Hz and an amplitude of 10μm, the tool's life improves to 98 grooves, indicating an approximate increase of 22%. Ibrahim et al. [109] conducted a comparison of tool wear between UVAMM and CMM. According to their study, applying a piezoelectric actuator to transmit small-scale vibrations and oscillating frequencies to the workpiece generates a tiny space that efficiently breaks down heat through the chip. Additionally, they discovered the complex tool path mechanism of 2D UVAMM, in which the proximity of the tool tip to the workpiece surface is influenced by the amplitude displacement along the applied frequency. By selecting the suitable amplitude and frequency, 2D UVAMM effectively minimizes tool wear and enhances surface roughness in comparison to CMM. Zheng et al. [50] investigated the process by

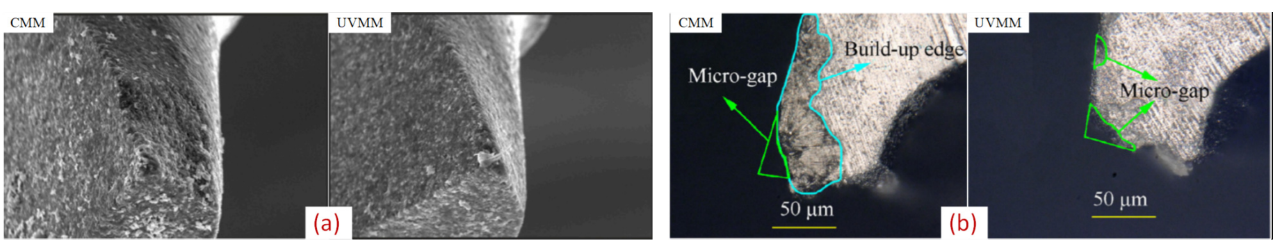

Fig. 19 Comparison of tool wear in CMM and UVMM (a) Greco et al. [51] (b) Fang et al. [82]

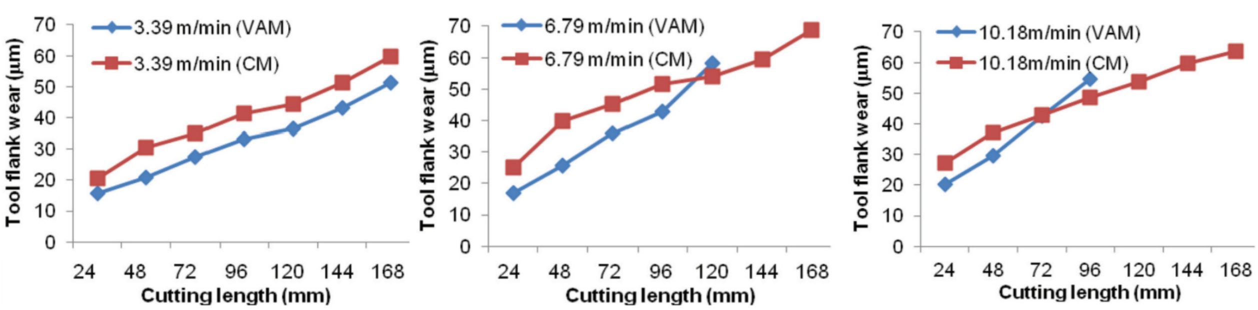

Fig. 20 Comparison of tool flank wear in CMM and UVAMM for different cutting length.

which tool wear is reduced in non-resonance-assisted micro-milling. They employed a coated micro-milling cutter to manufacture Ti6AL4V at three distinct vibration frequencies (high, medium, and low) after analyzing the tool's separation from the workpiece. The experiments focused on the cutting conditions, specifically if the tool was removed from the workpiece. Their findings showed that UVAMM efficiently reduces tool wear by employing various mechanisms which restrict wear. Li et al. [84] conducted a comparison of the tool wear in CMM and 2D UVAMM. The researchers discovered that the main characteristic of CMM tool wear is adhesive wear specifically occurring at the tip of the tool. Extended cutting operations, coupled with elevated temperatures and forces, may damage the cutting edge, resulting in a loss of its material-cutting capabilities. Conversely, the wear pattern of UVAMM shows notable differences. The material sticks to the edge of the cutting tool, resulting in adhesive wear. The phenomenon of micro-grinding occurs because of the cutting process, leading to a significant buildup of material on the side surface of the cutting edge. Subsequently, the material actively engages in the cutting procedure, so enhancing the quality of the surface. Li et al. [36] investigated the impact of tool wear on the tool life in UVAMM. It was discovered that increasing the cutting length had an impact on cutting performance when small amplitudes (2μm) were applied to microtools, namely due to tool flank wear. However, when the cutting speed is significantly lower than the maximum vibration speed, tool wear shows enhancement in comparison to CMM, but when the cutting speed and cutting length further increase, the ultrasonic vibration introduces additional vibrations and oscillations to the cutting process, causing the tool to experience greater forces and heat. These increased forces and heat can accelerate tool wear and result in shorter tool life, as shown in Fig. 20.

2.5. Cutting forces

During conventional cutting, the cutting forces are mainly affected by the machining dynamics, without the addition of any additional vibration assistance. The forces in discussion are frequently defined by the one-way movement of the cutting tool, leading to different force patterns [110]. Conversely, ultrasonic vibration cutting involves the introduction of dynamic oscillations during cutting. The periodic tool motions generated by ultrasonic vibrations impact the interaction between the tool and the workpiece. This results in a more complex distribution of force in comparison to conventional cutting processes. The combination of ultrasonic vibrations and conventional cutting forces alters the process of chip creation and impacts the mechanism of material removal. Hence, the addition of vibration can result in variations in cutting forces and, in certain instances, a decrease in the overall force generated on the tool, hence influencing tool wear and surface finish [111,112]. Shen et al. [113] found that while the maximum cutting force produced by UVAMM can sometimes be higher than that of CMM, the average cutting force of UVAMM is significantly lower. This observation remains valid for both experiments and finite element simulations. Interestingly, the variations in frequency and amplitude during UVAMM have significant effects on cutting forces. When the frequency increases from 0 Hz, it has a significant impact on reducing cutting forces. The reduction in forces caused by the resonance of the workpiece holder within this frequency range leads to a significant increase in vibrational amplitude and, consequently, a higher velocity of the workpiece under vibration. When frequency further increases from a range, the system is no longer excited by vibration, and the vibration amplitude decreases again, which results in an increase in the cutting force [52,85]. Similarly, when the amplitude increases from 0μm, the trajectory of tool tip 2 starts to be tangent to the trajectory of tool tip 1. This indicates that a cutting edge begins to intermittently cut during a cutting cycle, and chips break more effectively, ultimately reducing the cutting forces [76,108]. In addition, the further increase in amplitude can cause an increase in the cutting forces, which indicates that it is important to consider intermittent cutting conditions and impact force while choosing the amplitude. Fig. 21 illustrates the impact of tool vibration on cutting forces in UVAMM.

A comprehensive investigation has been carried out on the mechanisms and models of UVAMM cutting force generation and reduction. KIM et al. [12,114] investigated the V-groove's geometry and its impact on cutting forces in the UVAMM process. It was noted that the cutting force of UEVAMM were significantly reduced in comparison to conventional V-groove cutting, particularly when milling depths were smaller. It is important to mention that at a depth of 5μm, the cutting force of UEVAMM is reduced by a factor of four compared to the conventional approach. While the decrease in force is not as pronounced when milling at greater depths, such as 25 μm, UEVAMM still manages to achieve a 50% reduction in cutting force. This demonstrates that the decrease in force is more pronounced with the use of UEVAMM at lower milling depths. Researchers explain this phenomenon to the specific energy transfer mechanism of UEVAMM, which reduces the friction among the tool, chip, and workpiece. Fang and Yuan [76,82,108] conducted a comparison between simulated and experimental cutting forces in UVAMM and CMM. While the simulated values may somewhat exceed the actual forces, the general pattern of reduction in UVAMM cutting force remains constant. UVAMM effectively decreased all three force components (F_x, F_y, and F_z) in comparison to CMM, resulting in reductions ranging from 7.6% to 11.5%. In addition, they noted that a smaller vibration amplitude also had a significant impact on reducing cutting forces, and an increase in amplitude was more effective in reducing cutting forces due to the intermittent cutting effect. Xu et al. [43,115,116] conducted studies with and without vibration to directly compare the cutting forces in UVAMM and CMM. Their findings validated the effectiveness of UVAMM in reducing cutting forces on various workpiece materials, therefore enhancing machining precision and extending tool life. It is most important to note that the increase in amplitude from 0 μm to 4μm has a significant impact on reducing cutting forces, as shown in Fig. 22.

Hu et al. [117] investigated the unique function of ultrasonic torsional vibration (UTV) in decreasing cutting forces during ultrasonic torsional vibration-assisted micro milling (UTVAMM). Their investigations demonstrated that the primary cause for the observed decrease in force was the dynamic impact of torsional vibrations. Furthermore, they hold the belief that the feed per tooth is an important

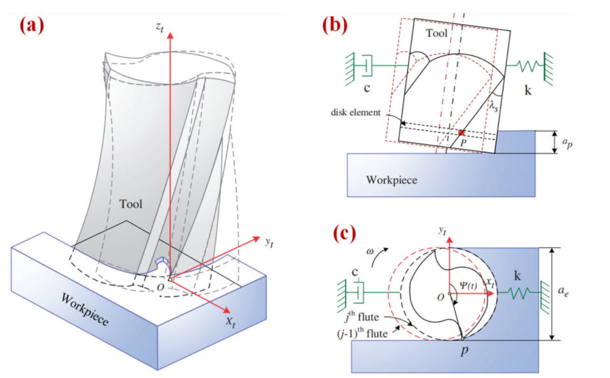

Fig. 21 Effects of the tool vibration on cutting forces.[73]

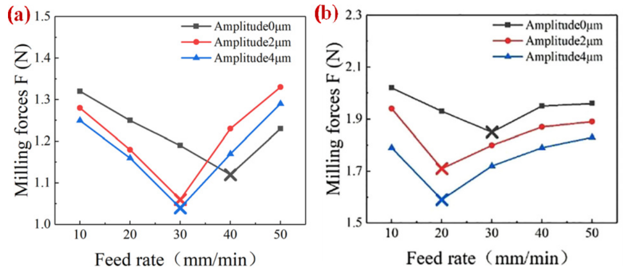

Fig. 22 Comparison of cutting forces in CMM and UVAMM (a) 6061T6 (b) TC4.

variable that influences the reduction of cutting force. They claim a smaller value of feed per tooth offers a better advantage in terms of cutting force reduction. Ding et al. [59,60] developed complex 3D cutting force models specifically for 2D UVAMM. Their model effectively predicted cutting forces across different situations by including the dynamic elements of the cutting process. The predicted forces exhibit a high level of agreement with the actual results, so confirming the precision of the model. Parenti et al. [118] also conducted a study on the decrease of cutting force in UVAMM. Huan et al. [53] conducted a comparison of the cutting forces between UEVAMM and CMM. The cutting speed was set at 30 m/min, and the vibration frequency was set at 20 kHz. It was noted that UEVAMM shows significant consistency because of its characteristics of vibration. During the milling process, the tool experiences stress concentration and extrusion, resulting in a substantial rise in cutting force. However, the UEVAMM exhibited a cutting force that was 60% lower than that of the CMM, as shown in Fig. 23(a). Greco et al. [51,52] conducted two separate investigations that showed the particular cutting force of UVAMM is much less than that of CMM. More precisely, the UVAMM force varies between 0.0016 and 0.0056 N/μm, whereas the CMM force varies between 0.011 and 0.082 N/μm, as shown in Fig. 23(b). In addition, when the frequency increases from 0 to 3.9 kHz, it helps reduce the cutting forces, but further increases in frequency again increase the cutting forces.

Zhang et al. [48] investigated the impact of vibration on cutting forces during the initial contact between the tool and the workpiece. They noticed that the application of vibration led to a rapid increase in cutting forces because of the initial impact upon contact. Subsequently, there is a significant decrease, demonstrating the discontinuous characteristic of the milling procedure in UVAMM. The discontinuous pattern of this behavior reduces the effectiveness of the side plow effect during up milling and causes the chips to break in advance, ultimately leading to lower average cutting forces compared to the CMM. Shang et al. [61,119] focused on developing 2D UVAMM cutting force models. The researchers studied multiple parameters that influence the instantaneous depth of cut, such as tool runout, size impacts, and cumulative effects. Subsequently, the model is employed to examine the impact of amplitude and frequency on cutting forces. Furthermore, they investigated the application of UVAMM for the objective of removing bone material throughout surgical processes, demonstrating the capability of this technology to reduce cutting forces and enhance the smoothness of bone surfaces during the milling process. Chen et al. [85] studied the overall cutting force characteristics in UVAMM. Frequent changes in the cutting force were noticed, and it was discovered that adding vibration at a frequency of 6 kHz resulted in a significant decrease in the average cutting force compared to the CMM. Their findings demonstrated that vibration can efficiently breakdown chips, thereby reducing total milling forces. Additionally, it was noted that as the vibration frequency increased, the average cutting force decreased even more. The most notable decrease was noticed at 60 kHz, which can be due to the obvious formation of material cracks, as shown in Fig. 24. Prabhu et al. [120] analyzed the distribution of cutting forces (F_x and F_y) during 2D UVAMM at varying increase frequencies (300 Hz and 600 Hz). Their findings demonstrated an inverse relationship between the generating frequency and the cutting force, whereby an increase in the earlier resulted in a decrease in the latter. Consequently, increasing the frequency at which the drive operates has the potential to enhance the performance of the machining process by reducing the forces exerted during cutting and improving the overall stability of the process.

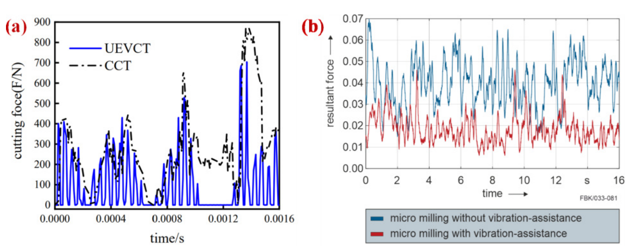

Fig. 23 Comparison of cutting forces in CMM and UVAMM (a) Huan et al. [53] (b) Greco et al. [52]

3.6. Cutting temperature

The temperatures produced during metalworking play an important role in determining the outcome of the cutting process in all its aspects. It significantly affects the wear and tear of tools, the formation of burrs, the mechanisms of chip removal, the quality of surfaces, the stress that remains, the deformation in three dimensions, and the accuracy of dimensions in microfeatures that have been machined [121-123]. The cutting temperature in conventional cutting techniques is mostly determined by the interaction between the tool and the workpiece during material removal. In conventional cutting, the cutting temperature typically rises because of the continuous and one-way cutting motion. This leads to the production of concentrated heat at the interface between the tool and the workpiece [124]. Meanwhile, UVAC generates dynamic oscillations when cutting. The tool experiences periodic engagement and disengagement with the workpiece due to ultrasonic vibrations, leading to discontinuous cutting action. The periodic process of tool engagement and disengagement leads to a distinct heat distribution in contrast to conventional cutting. By incorporating ultrasonic vibration, the dissipation of heat is enhanced, leading to a potential decrease in the overall cutting temperature [125,126]. Chen et al. [127] found that the introduction of ultrasonic vibration effectively enhances the diffusion time and space of cutting temperature. In addition, it is also evident from previous studies that the increase in amplitude and frequency has a significant impact on reducing cutting temperature [77]. Fig. 25 illus-

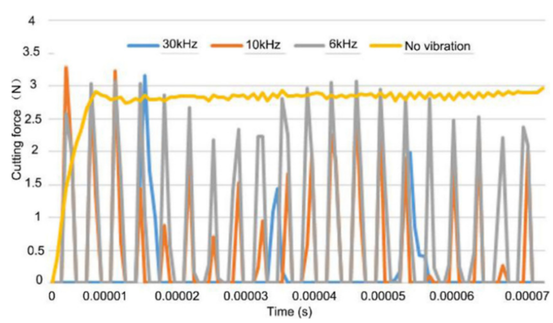

Fig. 24 Impact of frequency variations on cutting forces in UVAMM.[85]

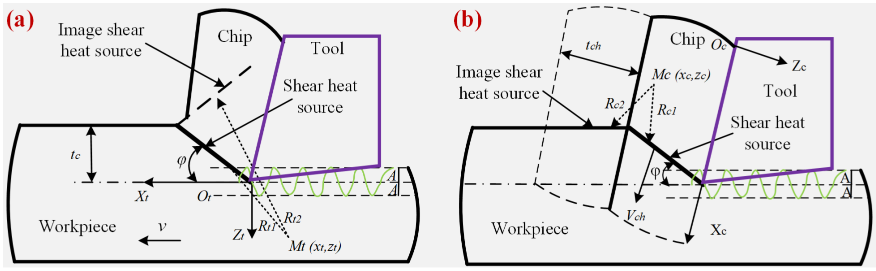

Fig. 25 Illustration of temperature generation in UVAM (a) Workpiece side heat source (b) Chip side heat source.[126]

trates the temperature modeling in UVAM.

While considerable attention has been devoted to the investigation of cutting temperature in CMM [128,129], the mechanisms determining the generation of cutting temperature in UVAMM remain unclear. Numerous scholars have initiated an investigation into this crucial element, offering significant perspectives into its behavior. Huan et al. [53] conducted a comparison of the cutting temperatures between CMM and UEVAMM and observed a significant decrease of 17.6% in the context of UEVAMM, as shown in Fig. 28. This reduction was attributed to the gap between the rake face and the workpiece during the vibration process, enabling the dissipation of heat. Conversely, the continuous interaction between the tool and workpiece in a CMM can result in the accumulation of heat and high temperatures.

Zhang et al. [48] investigated the distribution of the cutting temperature field in CMM and UVAMM. It was noted that the highest temperatures were found in the shear deformation zone and then gradually extended to other areas. UVAMM has a higher immediate cutting thickness compared to CMM, yet its intermittent nature minimizes the accumulation of heat. This minimizes the thermal energy produced due to friction between the tool and workpiece, allowing for enhanced cooling efficiency. Ibrahim et al. [109] conducted

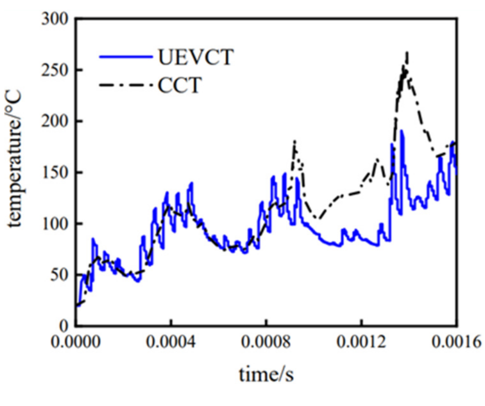

Fig. 26 Comparison of cutting temperature in CMM and UVAMM.

a comparison of cutting temperatures between UVAMM and CMM. The researchers observed the creation of small gaps because of applying low-amplitude and frequencies to the workpiece using a piezoelectric actuator. This space facilitates efficient heat dissipation of the chip. In addition, their research uncovered the complex mechanics of the tool path in 2D UVAMM. This involves how the proximity of the tool tip to the surface of the workpiece is influenced by the displacement amplitude at the given frequency. Shang et al. [77] investigated the use of UVAMM in orthopedic surgery, with a particular focus on bone milling. A temperature model was developed for vibration milling of bone materials and its accuracy has been verified by simulations. According to their research findings, UVAMM is more effective than CMM in reducing heat generation and minimizing thermal damage. In addition, the increase in amplitude from 0 to 4μm and frequency from 0 to 1000 Hz significantly reduced the temperature at the cutting zone, as shown in Fig. 27.

2.7. Surface morphology and roughness

The surface roughness of the machined surface is closely related to factors such as the structure of the micro milling tool, the accuracy of the machine tool, the amount of material being cut, the cooling conditions, and the wear of the tool. Choosing a lower feed rate may result in a reduction of the residual height of the machined surface if a smaller cutting edge radius is used [130]. Li and Chou [131] emphasized the significant impact of tool wear on surface roughness in micro milling, irrespective of the cutting conditions. The researchers discovered that by minimizing tool wear, it is possible to attain excellent surface quality in micro milling. According to Shaw [132], state that the surface generated by CMM is influenced by the accurate replication of the geometric and kinematic characteristics of the tool tip form factor. In addition, according to Ding et al. [60] state that in a CMM, the cutting tool would accurately replicate the tool profile on the machined surface as it moves along the actual tool path, thereby revealing the surface topography of the machined object. However, the 2D UVAMM exhibits circular motion properties that enable the cutting point of the tool to traverse the

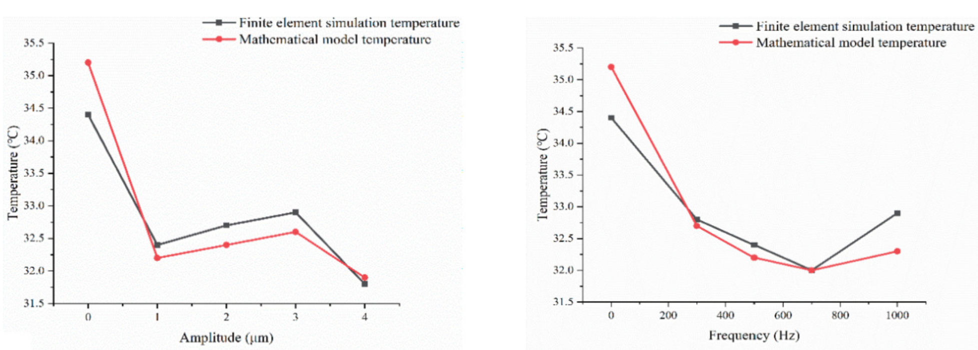

Fig. 27 Impact of amplitude and frequency variation on cutting temperature in UVAMM.[77]

cutting region of the preceding cycle, thereby eliminating the raised and lowered portions of material remaining from the previous cycle. The circular motion of the 2D UVAMM during the cutting process will minimize the impact of average force and enhance surface accuracy by reducing any vibrations between the tool and workpiece. In addition, when considering this viewpoint, decreasing the cutting forces of the tool also leads to a decrease in vibrations on the tool, so improving the quality of the surface produced [60,109]. Rasidi and Ding discovered that the utilization of 2D UVAMM facilitated the splitting of the machined surface into smaller parts. Simultaneously, these pieces are removed during alternating cycles by utilizing contrasting frequencies and amplitudes [133]. In addition, it is interesting to note from previous studies that the increase in amplitude[40,108] and frequency[104,116] decreases the surface roughness and improves the surface morphology of the cutting surface. Fig. 28 illustrates the development of surface topography in UVAM and Fig. 29 shows the machined surface in CMM and UVAMM.

Researchers have thoroughly investigated the impact of milling parameters on the surface integrity and quality of surfaces machined using UVAMM. Fang et al. [82] investigated the surface morphology of grooves that were machined using CMM and UVAMM. They noticed that surface defects gradually reduced when the feed per tooth (f_z) increased, particularly when the vibration amplitude was 0 μm. Defects are nearly removed when the value of f_z is 5 μm/z. Low f_z values result in excessive plastic deformation, causing the buildup and adherence of material, leading to the formation of burrs and defects in the surface. When ultrasonic vibration is applied with an amplitude of 3 μm and a frequency of 32 kHz, and a feed speed of 2 μm/z is maintained, the occurrence of pits, ridges, and grooves is significantly reduced. As the value of f_z increase, the

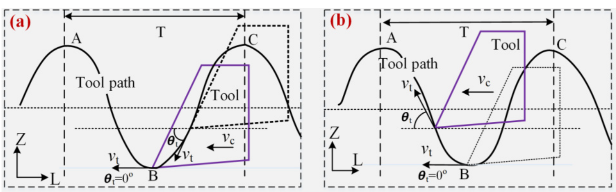

Fig. 28 Illustration of surface topography formation in UVAM[134] (a) 0-T/2 (b) T/2-T.

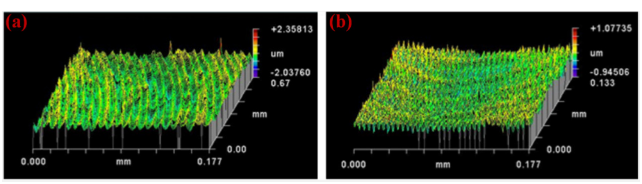

Fig. 29 Machined surface [104] (a) CMM (b) UVAMM.

surface roughness becomes more prominent. However, if the value of f_z reaches 5μm/z, the impact of ultrasonic vibration on surface quality becomes less pronounced. The decrease in defects is mostly related to the separation features of the vibration process, which impact the rate of change in the cutting process and the heating effect. Lian et al. [37] performed studies using three different ultrasonic vibration amplitudes to compare the surface quality of machined grooves with and without vibration. Their findings clearly demonstrate that surfaces subjected to UVAMM processing exhibit greater uniformity and absence of any machining marks, in contrast to surfaces treated with CMM causes micro defects. Chen et al. [71,72] investigated the development of various surface textures on the end face of the workpiece by using different combinations of machining and vibration parameters. The researchers suggested a technique for generating surface using a milling process that incorporates vibrations. They confirmed the efficiency of this method through experimental testing and showed that when the frequency increased from 0 to 3.4 kHz, the surface morphology improved. Guo Li et al. [84,95] conducted a study on the mechanism of surface development in 2D UVAMM. They also investigated how this mechanism affects chip removal efficiency, chip shape, and tool life. The researchers conducted experimental tests to confirm the accuracy of using vibration assistance to enhance the surface integrity and quality of machined surfaces. Their findings validated that the utilization of vibration assistance enhanced the micro step pattern on both surfaces of the thin-walled micro structured surface and altered the form of the groove's bottom because of tool eccentricity. Additionally, it was discovered that the vibration-assisted machined surface exhibited a shape deviation of less than 101 nm SPV and a surface roughness of less than 25 nm RMS. In addition, the increase in frequency from 2 to 10 kHz and amplitude from 0 to 4μm significantly reduces the surface roughness, as shown in Fig. 30. Li and Wang[36] investigated the correlation between surface roughness and cutting length in UVAMM and CMM. Upon reaching a milling length of 24 mm, the researchers saw that the rate of tool wear in both UVAMM and CMM became similar. Additionally, at this point, the surface roughness might be considered as an enhancement in the obtained surface quality by UVAMM. Thus, the extraordinary efficiency of UVAMM in the low-speed milling procedure was validated, resulting in a reduction in surface roughness by 56.4%, 4.4%, and 8.6% respectively for a milling length of 24 mm, as shown in Fig. 31.

Ibrahim et al. [38] discovered that at low frequencies, surface roughness increases as the frequency increases because of greater motion in the gap. However, within the ultrasonic frequency range, the surface roughness reduces because of the reduction in milling force and temperature. The increased frequency of vibration leads

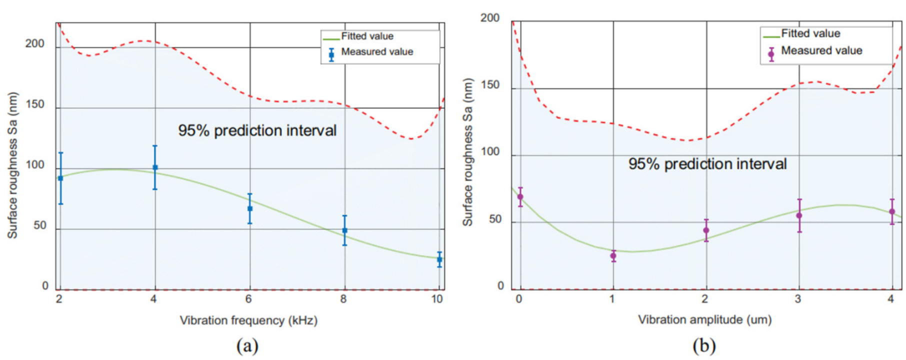

Fig. 30 Impact of vibration frequency and amplitude on surface roughness in UVAMM.[95]

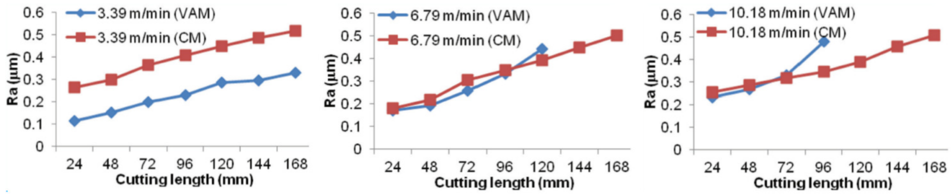

Fig. 31 Comparison of surface roughness in CMM and UVAMM.

to a significant enhancement in surface roughness caused by the increased gap between the cutting tool and the workpiece. This minimizes stress during the cutting process, enhancing cutting precision and lowering deformation, thereby decreasing the formation of burrs on the surface of the tool. Kiswanto et al. [135] proposed a theoretical model for surface roughness of UVAMM using the MATLAB software. This model accounts for the influence of the tool's bottom tip angle on the surface of the workpiece and can be employed to replicate the effects of UVAMM on the workpiece surface. Guo et al. [136] developed a machining system that utilizes vibrations to assist in the process. The system includes a worktable that is not resonant, allowing for the adjustment of the vibration frequency. The researchers conducted orthogonal experiments to investigate the impact of feed speed, vibration frequency, and amplitude on surface quality. Their findings shown that increasing the vibration frequency reduced the formation inaccuracy and roughness, whereas the amplitude enhanced the surface quality only within a particular range. The accuracy of a 3D surface shape simulation model of UVAMM developed by Yan et al. [40] was verified by experiments. The model offers valuable insights into the process of surface development under UVAMM, and the surface morphology improved on the cutting surface when the amplitude increased from 0 to 3μm. Xu et al. [43,116] reported that ultrasonic vibration decreased surface defects, leading to an enhancement in surface quality. In addition, they found a vibration-induced delay in the micro milling process and a reduction in surface roughness when the amplitude increased from 0 to 4μm, as shown in Fig. 32.

Tan et al. [54] conducted a comparison of the surface characteristics

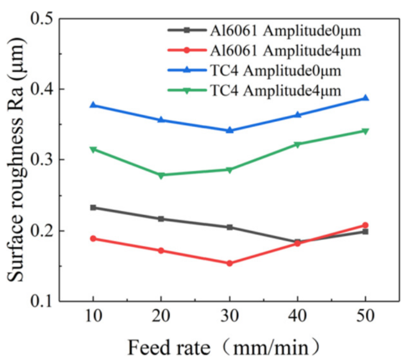

Fig. 32 Impact of amplitude on surface roughness in UVAMM.[43]

of microgrooves that were machined using CMM and UEVAMM. It was discovered that the CMM machined surface had surface defects such as ridges, cavities, and rip lines, but the UEVAMM machined surface had no such defects. Huan et al. [53] found that UEVAMM offered improved surface quality in comparison to CMM. The reduced surface roughness was due to the presence of movements nanoparticles in the matrix. Jin et al. [137] evaluated the impact of vibration direction, range, and frequency on surface roughness and profile in UVAMM. It was discovered that continuous vibration had the greatest effect in enhancing surface quality. Furthermore, the use of vibration assistance was discovered to improve the brittle transition of the glass film and reduce surface damage, as shown in Fig. 33(a). Du et al. [138] developed a comprehensive approach for predicting the vibration and surface roughness of micro-end mills. Their model addresses the accurate motions followed by the cutting edge, the vibrations of micro-end mills that depend on their size, and the elastic recovery of the material. The findings indicate that the vibration of micro-end mills leads to an increase in both micro-milling forces and surface roughness. This has been confirmed through experimental verification. Yuan et al. [76,108] studied the impact of UVAMM on surface quality by employing workpiece vibration machining. Their findings demonstrated that reducing milling speeds, feed rates, and employing moderate vibration amplitudes resulted in the most favorable surface morphology, as shown in Fig. 33(b). The morphology of this structure exhibits a consistent and symmetrical fish scale pattern, characterized by a smooth surface with minimum roughness and an absence of defects. Enhancing the surface quality was achieved by optimizing the cutting settings, namely by increasing the cutting speed to 37.68 m/min and adjusting the feed per tooth to 6μm. He et al. [74] introduced electrically assisted ultrasonic micromachining (EUMM) as a remedy for the issue of elevated surface roughness in workpieces. Their findings demonstrated that the implementation of EUMM led to a significant decrease in surface roughness. The EUMM method yielded a reduced bottom surface roughness (0.33 μm) compared to both the UVAMM and CMM methods. EUMM enhances the smoothness of the sidewalls by utilizing particles throughout the manufacturing process, resulting in a minimal surface roughness of 0.34 μm on the vertical sidewalls.

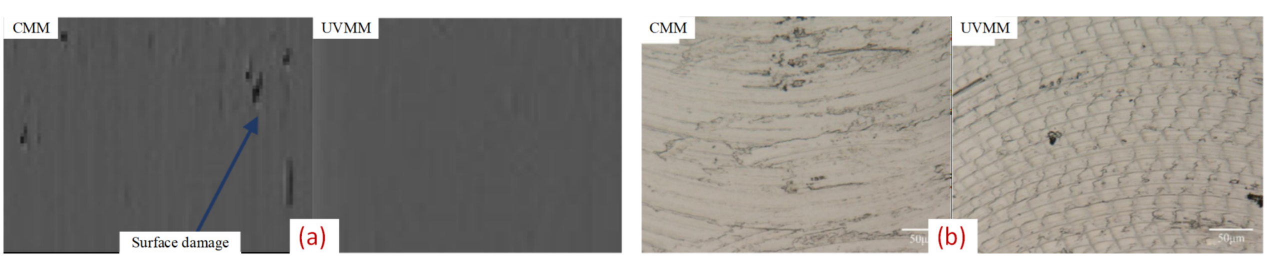

Fig. 33 Surface morphology comparison in CMM and UVMM (a) Jin et al. [137] (b) Yuan et al. [76]

3. Finite element simulation of machining process

The finite element approach is an effective tool for simulating the cutting process. When compared to physical testing, using this approach can greatly reduce costs and save time. It also enables the identification of an effective and practical production process at an early stage. Moreover, it offers useful perspectives on enhancing the characteristics of the cutting process. The progress in computer software and hardware has greatly improved the capabilities of finite element analysis (FEA) software, resulting in a major increase in research efficiency.

To study UVAMM mechanism and compare the results with CMM, many researchers have used ABAQUS [117] and Deform [48] software to develop detailed 2D and 3D finite element simulation models, which can be seen in Fig. 34.

Hu et al. [117] developed a thermomechanical coupled model of UVAMM using the ABAQUS software. This work offers significant insights into the role of feed per tooth in reducing cutting forces during the UTVAMM process. The research findings can be employed to enhance the UTVAMM process by increasing machining efficiency and minimizing tool wear. In another study, Hu et al. [139] developed a 2D finite element (FE) model of UVAMM using ABAQUS software. This study offers significant insights into the mechanism of UVAMM and the impact of process parameters on the performance of the manufacturing process. The results can be utilized to enhance the UVAMM process to optimize machining precision, surface quality, and reliability of micro-components. Chen et al. [85] developed a 2D FE model for the simulation of UEVAMM. This model simplifies the milling process by assuming that the workpiece keeps stationary while the micro milling cutter rotates. The simulation findings indicate that the elliptical vibration of the milling cutter leads to the formation of micro-texture on the milling surface. This study offers significant insights into the mechanism of UEVAMM and its prospective benefits for micro milling applications. In a subsequent study, Chen et al. [140] performed a comprehensive investigation of the fundamental milling process of UVAMM by combining FE simulation and experimental tests. A UVAMM FE model of magnesium alloy was created, employing the Johnson-Cook material model. Through an investigation of the size effect and material removal mechanism of UVAMM, it was determined that the vibration frequency has a substantial influence on the machining process. They found that by increasing the vibration frequency, they were able to successfully reduce burr formations, cutting forces, and tool wear. The accuracy of these discoveries is supported by the results of finite element simulation and experimental validation. Zheng et al. [50] utilized FE simulation and experimental techniques to investigate the mechanism of tool wear reduction in non-resonance-assisted micro-milling. A UVAMM FE model was developed using the ABAQUS software, which integrated a Johnson-Cook material model and a damage model. The results show that UVAMM is highly successful in minimizing tool wear by employing numerous mechanisms that prevent wear. Zhang et al. [48] developed a 3D FE model using Deform software to investigated the mechanism of burr formation in CMM and UVAMM. They subsequently carried out experiments to validate their findings. According to their research, the application of high-frequency ultrasonic vibration in the milling feed direction can successfully decrease cutting temperature and forces, enhance chip breaking capability, and thus minimize the burr formation. The experimental results further validated the precision of the simulation results and offered useful parameter guidance. Huan et al. [53] investigated the cutting characteristics of ultrasonic vibration using a 2D thermodynamic coupled finite element milling model. The researchers discovered that ultrasonic elliptical vibration cutting outperformed conventional cutting in terms of surface profile, average milling force, and milling temperature, as presented in Fig. 35. During the cutting process, the stress is generally applied horizontally, and the removal of material particles primarily occurs through cutting.

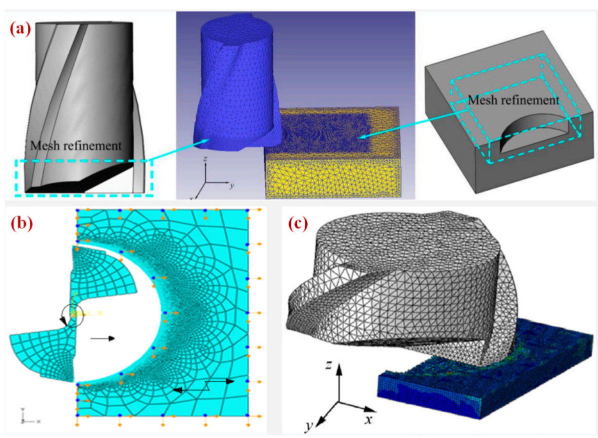

Fig. 34 Finite element simulation models (a) Deform 3D model (b) ABAQUS 2D model (c) ABAQUS 3D model.

Fang et al. [82] highlighted the application of FE simulations for the prediction of cutting forces. The milling forces derived from simulations and experiments were effectively compared, thus confirming the accuracy of the model. Lu et al. [141] developed a 2D FE model of UVAMM using ABAQUS software. Their approach integrates the Johnson-Cook flow stress model and shear failure principles of the workpiece material, along with the modified Coulomb friction law that includes both sliding and bonded components. The researchers conducted a study using FEA to investigate the impact of cutting parameters, vibration parameters, and tool shape on the process. Furthermore, they conducted an analysis of the residual levels of stress in various tool flank wear conditions, offering useful insights for the enhancement of process parameters, the improvement of product performance, and the optimization of tool life and reliability. Shang et al. [77] developed a 3D FE temperature model using ABAQUS software for bone material in UVAMM and compared with CMM, as shown in Fig. 36. The validity of their

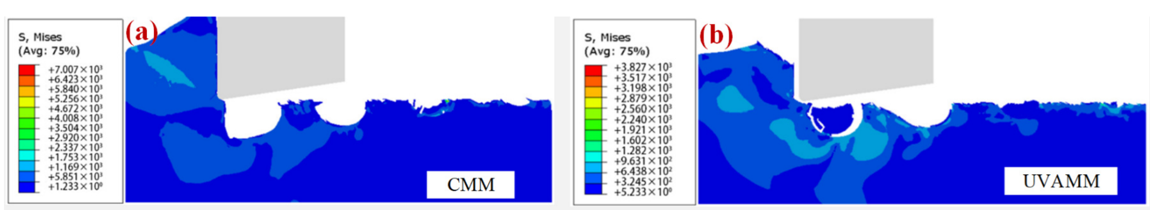

Fig. 35 Surface morphology by FEA (a) CMM (b) UVAMM.

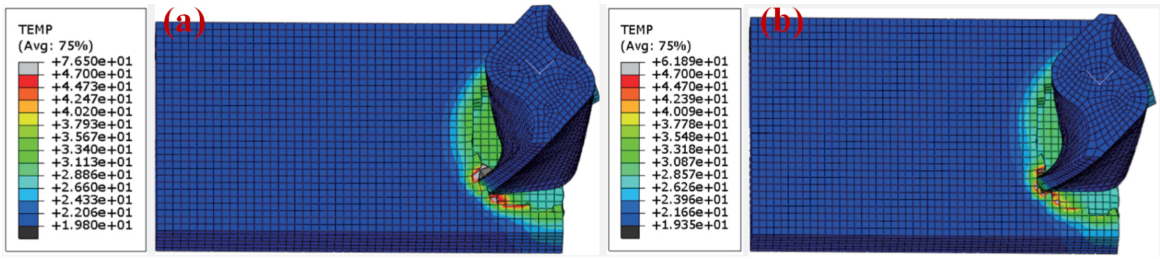

Fig. 36 Temperature nephogram of bone material by FEA (a) CMM (b) UVAMM.

model was confirmed using FEA simulations, emphasizing the potential of FEA in examining thermal behavior in UVAMM applications.

4. Significance of MQL in UVAMM

The main goal of employing cooling lubricants in machining is to enhance the quality and efficiency of the final products. Studies have demonstrated that the use of significant coolants and lubricants can enhance surface quality, reduce tool deterioration, and minimize cutting forces. In addition, they assist in minimizing thermal deformation, hence enhancing the precision of the design and ability to remove chips [142,143]. Although conventional cooling lubricants offer numerous advantages, they represent an important challenge due to their negative impact on the environment and human health. As a result, there has been a growing focus on the development of eco-friendly alternatives, such as minimum quantity lubrication (MQL), and cryogenic cooling [144]. In MQL, a small quantity of lubricant is directed toward the cutting zone in the presence of air [145].

Only two studies were conducted in UVAMM by applying the MQL, and they showed a significant impact of the MQL on machinability improvement. Hence, additional study is necessary to fully understand and maximize its potential advantages in UVAMM. Li and Wang[36] investigated the impact of MQL on tool wear during UVAMM and made a comparison with dry cutting. Their findings show that the utilization of MQL significantly reduced tool wear, thus improving cutting performance in relation to surface roughness and the formation of burrs, as shown in Fig. 37. Ibrahim et al. [38] conducted research to investigate the impact of MQL on the processing performance of UVAMM. It was noted that the use of UVAMM alone enhanced the quality of machining, but the addition of MQL resulted in further improvements in mechanical accuracy. This implies that MQL can enhance the beneficial impact of UVAMM on dimensional precision, leading to improved machining results.

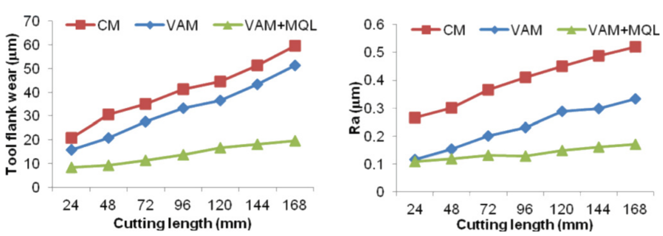

Fig. 37 Significance of MQL in UVAMM.

5. Advantages of UVAMM for difficult-to-cut materials

UVAMM is an innovative machining technique that uses CMM with high-frequency vibration. UVAMM offers outstanding versatility beyond its ability to manage complex geometries. The versatility of this method is seen in its extensive compatibility with difficult-to-cut materials, such as titanium alloys [84], steel alloys [104], nickel-based alloys [108], aluminum alloys [61], composites [116], brass [52], and optical glass [137]. Fig. 38 summarizes the properties that make these materials difficult to cut. In addition, these materials are widely used in biomedicine, optics, aerospace, semiconductors, and other fields because they have excellent physical, chemical, and mechanical properties [146-152]. Based on research, it can be found that published reports mainly focus on cutting characteristics, cutting forces, surface quality, and subsurface damage. Compared with CMM, UVAMM has shown good performance, as presented in Table 2. This compatibility allows for the efficient manufacturing of high-quality products.

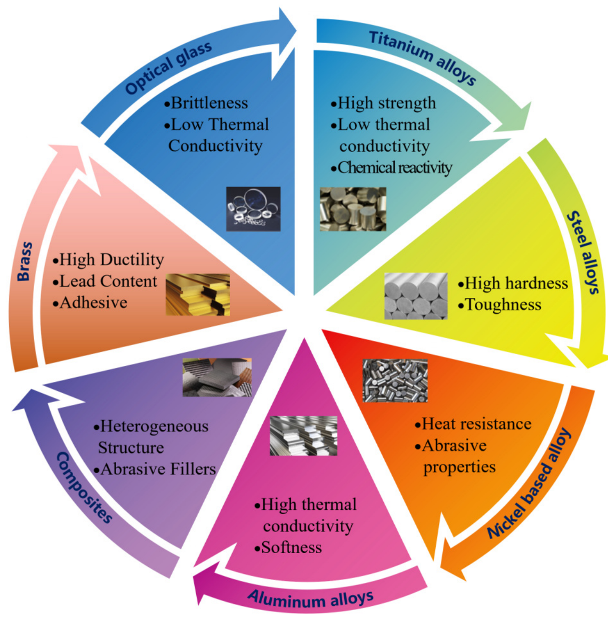

Fig. 38 Properties of the materials that make them difficult to cut.[146-152]

6. Conclusion

This article presents a comprehensive review of the latest developments in ultrasonic vibration-assisted micro-milling (UVAMM). It specifically focuses on various aspects, such as UVAMM processing, which include mathematical modeling, chip formation, burr formation, tool wear, cutting forces, cutting temperature, and surface morphology; the finite element simulation of UVAMM; the significance of MQL in UVAMM; and applications of UVAMM for difficult-to-cut materials such as titanium alloys, steel alloys, nickel-based alloys, aluminum alloys, composites, brass, and glass. The following possible conclusions can be drawn from this review:

(1) Micro-milling demonstrates exceptional proficiency in creating complex 3D shapes on various materials, although it encounters

multiple challenges when it comes to difficult-to-machine materials. UVAMM is a promising technology that can effectively tackle these challenges while achieving a wide range of applications for difficult-to-machine materials.

(2) UVAMM improves chip breaking properties, reduces burr formation by creating variations in chip thickness across different regions, and promotes natural breakage.

(3) UVAMM effectively addresses the issues related to tool wear, cutting forces, cutting temperature, and surface roughness encountered while machining challenging materials. By conducting experiments and utilizing models, we may make precise predictions and optimize these factors to attain exceptional outcomes. The periodic cutting movement produced by UVAMM vibration enhances the service life of the tool, reduces forces and temperatures, and enhances the quality of the surface finish.

(4) Advancements in hardware and software have pushed finite element analysis (FEA) to unprecedented levels, greatly enhancing research productivity. The FEA model developed by UVAMM also exhibited enhanced precision, offering important insights into the improvement of the process.

(5) The UVAMM has great potential on its own, and the addition of MQL further enhances its overall efficiency, establishing it as an effective strategy for achieving precise micromachining.

(6) UVAMM demonstrated its versatility by smoothly working with a diverse range of materials, such as titanium alloys, steel alloys, nickel-based alloys, aluminum alloys, composite materials, brass, and optical glass. This adaptability allows to produce better products that enhances efficiency across numerous applications.

Table 2 Research summary of the difficult-to-cut materials in UVAMM.

No.	Authors	Materials	Vibration type	Improvements compared with CMM
1	Greco et al. [52]	Brass (CuZn39Pb2)	1D	The comparison with CMM revealed a substantial 63% decrease in cutting forces, reduced burr formation, and improved surface quality, indicating the potential of UVAMM to enhance efficiency.
2	Fang et al. [82]	Inconel718	1D	The UVAMM helps to reduce feeding force (F_x), radial force (F_y), and axial force (F_z) up to 7.6%, 11.5%, and 1.3%, respectively, and optimize surface quality and burr suppression.
3	Xu et al. [116]	Graphene-based aluminum matrix composite	1D	These composites showed excellent processing characteristics when subjected to precise feed rate and ultrasonic amplitude conditions (1μm/tooth and 3.05μm, respectively). This shows the capacity to optimize UVAMM parameters to attain higher outcomes for composite materials.
4	Li et al. [95]	Al6061 aluminum alloy	1D	Findings offered proof of the ability of UVAMM to enhance surface integrity and quality. Their study also investigated the impact of vibration frequency and amplitude on surface roughness and burr size. They discovered a positive correlation between surface roughness and frequency, as well as a negative correlation between surface roughness and amplitude.
5	Greco et al. [51]	AISI 316L	1D	Investigated the effects of vibration assistance on tool wear, cutting forces, surface roughness, and burr formation. The results show the reduction in tool wear, cutting forces, surface roughness and burr formation demonstrating the efficiency of UVAMM.
6	Xu et al. [43]	TC4 titanium alloy and 6061T6 aluminum alloy	1D	The findings demonstrated that employing ultrasonic vibration resulted in a significant 17% and 12% reduction in cutting forces for titanium alloy TC4 and aluminum alloy 6061T6, respectively, when compared to the CMM.
7	Han et al. [96]	304 austenitic stainless steel	1D	The experimental results show that horizontal ultrasonic vibrations can change the morphology of the burr, transforming it from an elongated form to a continuous sheet-like structure that results in an improvement in surface finish in micro grooves.
8	Yuan et al. [108]	Inconel718	1D	In this investigation, UVAMM and CMM were compared, with a particular focus on cutting forces, tool wear, surface morphology, and corrosion resistance. The results show that UVAMM reduces cutting forces, leading to exceptional surface quality. Furthermore, the application of ultrasonic vibration greatly improves the surface corrosion resistance of Inconel 718.
9	Yuan et al. [78]	Inconel718	1D	The results demonstrated that UVAMM enhances chip breakdown, promotes the development of burr cracks, and efficiently reduces burr formation.
10	Zhang et al. [48]	Inconel718	1D	Simulation and experimental results proved that applying high-frequency ultrasonic vibration in the milling feed direction reduces cutting temperature and cutting force, improves chip breaking ability, and reduces burr formation.

Continued table 2

No.	Authors	Materials	Vibration type	Improvements compared with CMM
11	Zhang et al. [73]	Al6061 aluminum alloy	1D	Researchers experimentally verified a dynamic cutting force model for micro-end milling of Al6061. This model considers tool vibration and runout. Their model demonstrated greater precision compared to conventional models and effectively predicted and comprehended cutting forces in UVAMM processes.
12	Xu et al. [115]	45# steel	1D	The researchers conducted orthogonal experiments to investigate the impact of grain size and ultrasonic vibration on cutting forces, dimensional accuracy, and surface roughness. Their findings showed that materials with larger grain sizes tend to exhibit reduced cutting forces and attain improved surface quality when subjected to same process parameters.
13	Jin and Xie [137]	BK-7 optical glass	1D	The researchers conducted a series of tests to investigate the impact of vibration direction, amplitude, and frequency on surface roughness and profile. Their findings indicated that frequently utilized vibrations play an important role in enhancing the quality of the surface, offering helpful insight for optimizing parameters of UVAMM in the processing of optical glass.
14	Li et al. [84]	Ti-6Al-4V titanium alloy	2D	The researchers conducted a comparative analysis of the effects of UVAMM and CMM on both the structural integrity and quality of the parts. Their research aimed to develop an efficient UVAMM system for cutting the bottom surface of micro-grooves.
15	Ding et al. [104]	Tool steels of HRC 55 and HRC 58	2D	Experiments that explored how vibration parameters affected surface roughness and tool wear showed that using UVAMM can improve surface finish and lower tool wear compared to CMM.
16	Shang et al. [61]	Al6061 aluminum alloy	2D	Researcher developed and experimentally verified a 2D UVAMM to predict the cutting forces of Al6061. Their model accurately replicated cutting force curves and provided valuable insights into the impact of vibration amplitude and frequency on cutting forces.
17	Huan et al. [53]	TiC Particle-Reinforced Titanium Matrix Composites	2D	The ABAQUS simulation software was used to study the changes in cutting force, temperature, and processing conditions in the context of the CMM and UEVAMM processes. Their study evaluated the resultant surface morphologies and particle dispersion providing useful insights on the efficiency of UEVAMM on composites.
18	Yan et al. [40]	TC4 titanium alloy	2D	Researchers develop reliable predictive models of 3D machined surface morphology for the TC4 titanium alloy. The 3D surface morphology of the machined surface under LUVAM was simulated, and LUVAM experiments were conducted to explore the influence of processing parameters on surface morphology through simulation and experimentation. The results show that the simulation results are consistent with the experimental results, verifying the accuracy and reliability of the theoretical model.
19	Su et al. [79]	TC4 titanium alloy	3D	When compared to CMM, longitudinal-torsional ultrasonic-assisted and tangential torsion-assisted ultrasonic spiral-assisted processing had the fewest burrs, the smoothest surfaces, the largest fractal dimensions, and the least micro-milling force.

7. Research trends

Ultrasonic vibration-assisted micro-milling (UVAMM) is a developing field of research with a focus on reducing cutting force, improving tool life, improving surface quality, optimizing machining efficiency, and expanding its capabilities to the manufacturing industry. The research trend in UVAMM is focused on several key areas:

(1) A major focus is on finding the optimal combination of ultrasonic vibration parameters (amplitude, frequency) and conventional cutting parameters (cutting speed, feed rate) for different materials. This research often involves using simulations and experimental verification to identify settings that minimize cutting forces, improve surface quality, and extend tool life.

(2) The research focus is also increasing to explore the impact of combined vibrations of the tool and workpiece on the machining performance to improve efficiency as compared to applying vibrations only to the tool or workpiece.

(3) Researchers are exploring the combination of ultrasonic vibration with other micro-milling techniques like cryogenic cooling

or the use of specific cutting tool geometries to achieve even better results. Cryogenic cooling, for instance, can further reduce heat generation, potentially improving the machinability of heat-sensitive materials. It is exploring how ultrasonic vibration can be used to reduce cutting forces and tool wear, ultimately leading to less energy consumption and a lower overall environmental impact.

(4) A well-designed ultrasonic vibration-assisted device plays an important role in improving efficiency. Therefore, the researchers have focused on optimizing the design of the ultrasonic device to achieve higher efficiency in UVAMM.

(5) The interest in using UVAMM for machining novel materials that are difficult to process with conventional techniques is increasing. This includes research on the machining of composite materials, high-strength alloys, and even hard-to-cut biomaterials for medical applications.

(6) The research focuses on sustainable micro-milling due to growing environmental concerns. It is exploring how ultrasonic vibration can be used to reduce cutting forces and tool wear, ultimately leading to less energy consumption and a lower overall environmental impact.

Acknowledgment

This work was supported by the National Natural Science Foundation of China (Nos. 52375400 and 51975053), Independent Innovation and Special Funding Project (No. ZZCX-2023-029), Basic Research Foundation of Beijing Institute of Technology (No. 2021CX01023).

References

1. Wu X, Li L, He N. Investigation on the burr formation mechanism in micro cutting. *Precis Eng*. 2017;47:191-196.
2. Masato D, Sorgato M, Parenti P, et al. Impact of deep cores surface topography generated by micro milling on the demolding force in micro injection molding. *J Mater Process Tech*. 2017;246:211-223.
3. Cheng X, Nakamoto K, Sugai M, et al. Manufacturing Technology Development of ultra-precision machining system with unique wire EDM tool fabrication system for micro / nano-machining. *CIRP Ann*. 2008; 57:415-420.
4. Cheng X, Wang ZG, Nakamoto K, et al. Design and development of a micro polycrystalline diamond ball end mill for micro/nano freeform machining of hard and brittle materials. *J Micromechanics Microengineering*. 2009;19(11).
5. Suzuki H, Moriwaki T, Yamamoto Y, et al. Precision cutting of aspherical ceramic molds with micro PCD milling tool. *CIRP Ann - Manuf Technol*. 2007;56(1):131-134.
6. Zhang Z, Peng H, Yan J. Micro-cutting characteristics of EDM fabricated high-precision polycrystalline diamond tools. *Int J Mach Tools Manuf*. 2013;65:99-106.
7. Heaney PJ, Sumant A V, Torres CD, et al. Diamond coatings for micro end mills: Enabling the dry machining of aluminum at the micro-scale. Diam Relat Mater. 2008;17:223-233.
8. Cai Y, Liu Z, Shi Z, et al. Optimum end milling tool path and machining parameters for micro Laval nozzle manufacturing. *J Eng Manuf*. 2015;(1-10).
9. Liang Z, Gao P, Wang X, et al. Cutting performance of different coated micro end mills in machining of Ti-6Al-4V. *Micromachines*. 2018;9 (11):568.
10. Alhadeff LL, Marshall MB, Curtis DT, et al. Protocol for tool wear measurement in micro-milling. *Wear*. 2019;420-421(November 2018): 54-67.
11. Vipindas K, Kuriachen B, Mathew J. Investigations into the effect of process parameters on surface roughness and burr formation during micro end milling of TI-6AL-4V. *Int J Adv Manuf Technol*. 2019;100(5-8):1207-1222.
12. Kim GD, Loh BG. An ultrasonic elliptical vibration cutting device for micro V-groove machining: Kinematical analysis and micro V-groove machining characteristics. *J Mater Process Technol*. 2007; 190(1-3): 181-188.
13. Weng F, Liu Y, Chew Y, et al. IN100 Ni-based superalloy fabricated by micro-laser aided additive manufacturing: Correlation of the microstructure and fracture mechanism. *Mater Sci Eng A*. 2020;788:139467.
14. Allegre OJ, Li Z, Li L. Tailored laser vector fields for high-precision micro-manufacturing. *CIRP Ann*. 2019;68(1):193-196.
15. Cadot GBJ, Axinte DA, Billingham J. Continuous trench, pulsed laser ablation for micro-machining applications. *Int J Mach Tools Manuf*. 2016;107:8-20.
16. Derevyanko DI, Shelkovnikov VV, Orlova NA, et al. Fabrication of High-aspect-ratio Microstructures for LIGA-technology by Sinchrotron Radiation Polymerisation of Thetetraacrylate Monomer. *Phys Procedia*. 2017;86(June 2015):122-126.
17. Ma Y, Liu W, Liu C. Research on the process of fabricating a multilayer metal micro-structure based on UV-LIGA overlay technology. *Nanotechnol Precis Eng*. 2019;2(2):83-88.
18. Hamdana G, Puranto P, Langfahl-Klabes J, et al. Nanoindentation of crystalline silicon pillars fabricated by soft UV nanoimprint lithography and cryogenic deep reactive ion etching. *Sensors Actuators, A Phys*. 2018;283:65-78.
19. Bogaerts W, Dumon P, Taillaert D, et al. SOI nanophotonic waveguide structures fabricated with deep UV lithography. *Photonics Nanostructures - Fundam Appl*. 2004;2(2):81-86.
20. Wang K, Zhang Q, Zhang J. Evaluation of scale effect of micro electrical discharge machining system. *J Manuf Process*. 2019;38(November 2017):174-178.
21. Kim YS, Chu CN. The Effects of graphite powder on tool wear in micro electrical discharge machining. *Procedia CIRP*. 2018; 68(April): 553-558.
22. Kuzin V V, Fedorov SY, Szalay T, et al. Micromachining of a high-density current-conducting ceramic with the use of electrical-discharge machining. Part 2. *Refract Ind Ceram*. 2016;57(3):283-287.
23. Silvestre CM, Nguyen V, Jansen H, et al. Deep reactive ion etching of 'grass-free' widely-spaced periodic 2D arrays, using sacrificial structures. *Microelectron Eng*. 2020;223:111228.
24. Li Y, Zhang H, Yang R, et al. In-plane silicon microneedles with open capillary microfluidic networks by deep reactive ion etching and sacrificial layer based sharpening. *Sensors Actuators, A Phys*. 2019; 292: 149-157.
25. Sahoo P, Patra K, Szalay T, et al. Determination of minimum uncut chip thickness and size effects in micro-milling of P-20 die steel using surface quality and process signal parameters. *Int J Adv Manuf Technol*. 2020;106(11-12):4675-4691.
26. Ren Y, Li C, Li W, et al. Study on micro-grinding quality in micro-grinding tool for single crystal silicon. *J Manuf Process*. 2019; 42 (May):246-256.
27. Leo Kumar SP. Measurement and uncertainty analysis of surface roughness and material removal rate in micro turning operation and process parameters optimization. *Meas J Int Meas Confed*. 2019; 140: 538-547.
28. Suresh N, Ganesh S, Jagadesh T. Investigations into edge radius and point angle on energy consumption during micro drilling of titanium alloy. *Mater Today Proc*. 2019;26:586-591.
29. Liao Z, Axinte DA. On monitoring chip formation, penetration depth and cutting malfunctions in bone micro-drilling via acoustic emission. *J Mater Process Technol*. 2016;229:82-93.
30. Brehl DE, Dow TA. Review of vibration-assisted machining. *Precis Eng*. 2008;32(3):153-172.
31. Babitsky VI, Kalashnikov AN, Meadows A, et al. Ultrasonically assisted turning of aviation materials. *J Mater Process Technol*. 2003;132(1-3):157-167.
32. Suárez A, Veiga F, de Lacalle LNL, et al. Effects of Ultrasonics-Assisted Face Milling on Surface Integrity and Fatigue Life of Ni-Alloy 718.

J Mater Eng Perform. 2016;25(11):5076-5086.
33. BIE Wenbo, Bo Z, Fan C, et al. Progress of ultrasonic vibration-assisted machining surface micro-texture and serviceability. *Diam Abrasives Eng Aug*. 2023;43(No. 4).
34. Chern GL, Chang YC. Using two-dimensional vibration cutting for micro-milling. *Int J Mach Tools Manuf*. 2006;46(6):659-666.
35. Chen W, Teng X, Zheng L, et al. Burr reduction mechanism in vibration-assisted micro milling. *Manuf Lett*. 2018;16:6-9.
36. Li KM, Wang SL. Effect of tool wear in ultrasonic vibration-assisted micro-milling. *Proc Inst Mech Eng Part B J Eng Manuf*. 2014;228(6): 847-855.
37. Lian H, Guo Z, Huang Z, et al. Experimental research of Al6061 on ultrasonic vibration assisted micro-milling. *Procedia CIRP*. 2013;6:561-564.
38. Ibrahim R, Rahim EA, Ibrahim AA, et al. The effect on the application of coolant and Ultrasonic Vibration Assisted Micro Milling on machining performance. *Applied Mechanics and Materials* 2014;660:65-69.
39. Mokhtari A, Jalili MM, Mazidi A, Abootorabi MM. European Journal of Mechanics / A Solids Size dependent vibration analysis of micro-milling operations with process damping and structural nonlinearities. *Eur J Mech / A Solids*. 2019;76(August 2018):57-69.
40. Yan Y, Jiang C, Yan H. Probabilistic model of the surface residual height under longitudinal - torsional ultrasonic vibration assisted micro - milling TC4. *Int J Adv Manuf Technol*. 2024;131(5-6):2837-2855.
41. Özel T, Olleak A, Thepsonthi T. Micro milling of titanium alloy Ti-6Al-4V: 3-D finite element modeling for prediction of chip flow and burr formation. *Prod Eng*. 2017;11(4-5):435-444.
42. Teng X, Huo D, Shyha I, et al. An experimental study on tool wear behaviour in micro milling of nano Mg / Ti metal matrix composites. *International Journal of Advanced Manufacturing Technology* 2018: 2127-2140.
43. Xu LH, Na HB, Han GC. Machinablity improvement with ultrasonic vibration-assisted micro-milling. *Adv Mech Eng*. 2018;10(12):1-12.
44. Huo D, Lin C, Choong ZJ, et al. Surface and subsurface characterisation in micro-milling of monocrystalline silicon. *Int J Adv Manuf Technol*. 2015;81(5-8):1319-1331.
45. Dadgari A, Huo D, Swailes D. Investigation on tool wear and tool life prediction in micro-milling of Ti-6Al-4V. *Nanotechnol Precis Eng*. 2018;1(4):218-225.
46. Huo D, Lin C, Dalgarno K. An experimental investigation on micro machining of fine-grained graphite. *Int J Adv Manuf Technol*. 2014;72 (5-8):943-953.
47. Kiswanto G, Johan YR, Poly, et al.. *IOP Conf Ser Mater Sci Eng*. 2019;654(1):012012.
48. Zhang Y, Yuan Z, Fang B, et al. Study on the mechanism of burr formation by simulation and experiment in ultrasonic vibration-assisted micromilling. *Micromachines*. 2023;14(3):625.
49. Ding H, Chen SJ, Ibrahim R, et al. Investigation of the size effect on burr formation in two-dimensional vibration-assisted micro end milling. *P I Mech Eeg B-J Een*. 2011;225(B11):2032-2039.
50. Zheng L, Chen W, Huo D. Investigation on the tool wear suppression mechanism in non-resonant vibration-assisted micro milling. *Micromachines*. 2020;11(4):380.
51. Greco S, Klauer K, Kirsch B, et al. Vibration-assisted micro milling of AISI 316L produced by laser-based powder bed fusion. *J Manuf Process*. 2021;71(June):298-305.
52. Greco S, Kirsch B, Aurich JC. Simulation and application of a piezo-driven system enabling vibration-assisted micro milling. 2*nd International Conference of the DFG International Research Training Group 2057 - Physical Modeling for Virtual Manufacturing*. 2021; 89(3):3:1-3:0.
53. Huan H, Xu W, Zhao B, et al. Simulation study of ultrasonic elliptical vibration cutting of TiC particle-reinforced titanium matrix composites. *Metals (Basel)*. 2022;12(10):1-13.
54. Tan R，Zhao X，Sun T，et al. Experimental Investigation on micro-groove manufacturing of Ti-6Al-4V alloy by using ultrasonic elliptical vibration assisted cutting. *Materials (Basel)*. 2019;12(19):3086.
55. Chen X, Tang J, Shao W, et al. An analytical and experimental study on cutting characteristics and transient cutting force modeling in feed directional ultrasonic vibration-assisted cutting of high strength alloys. *Materials (Basel)*. 2022;15(20).
56. Rinck PM, Gueray A, Zaeh MF. Modeling of cutting forces in 1-D and 2-D ultrasonic vibration-assisted milling of Ti-6Al-4V. *Int J Adv Manuf Technol*. 2022;119(3-4):1807-1819.
57. Jin X, Poudel A. 1712 . Experimental study on high frequency chatter attenuation in 2-D vibration assisted micro milling process. *J Vibroeng* 2015;17(6):2743-2754.
58. Ma L, Howard I, Pang M, et al. Experimental investigation of cutting vibration during micro-end-milling of the straight groove. *Micromachines*. 2020;11(5):494.
59. Ding H, Chen SJ, Cheng K. Two-dimensional vibration-assisted micro end milling: Cutting force modelling and machining process dynamics. *Proc Inst Mech Eng Part B J Eng Manuf*. 2010; 224(12): 1775-1783.
60. Ding H, Chen SJ, Cheng K. Dynamic surface generation modeling of two-dimensional vibration-assisted micro-end-milling. *Int J Adv Manuf Technol*. 2011;53(9-12):1075-1079.
61. Shang P, Huang S, Liu X. Modeling and experimental study on cutting forces of 2D vibration assisted micro-milling. *China Mech Eng*. 2021; 32(6):648-657.
62. Rinck PM, Gueray A, Kleinwort R, et al. Experimental investigations on longitudinal-torsional vibration-assisted milling of Ti-6Al-4V. *Int J Adv Manuf Technol*. 2020;108(11-12):3607-3618.
63. Balázs BZ, Geier N, Takács M, et al. A review on micro-milling: recent advances and future trends. *Int J Adv Manuf Technol*. 2021;112(3-4):655-684.
64. Li P. *Micromilling of hardened tool steels*. *mechanical maritime & materials engineering*. 2009.
65. Dib MHM, Duduch JG, Jasinevicius RG. Minimum chip thickness determination by means of cutting force signal in micro endmilling. *Precis Eng*. 2018;51(August 2017):244-262.
66. Son SM, Lim HS, Ahn JH. Effects of the friction coefficient on the minimum cutting thickness in micro cutting. *Int J Mach Tools Manuf*. 2005;45(4-5):529-535.
67. Zhang Y, Zhang Q, Zhao J, et al. Ultrasonic vibration assisted milling of titanium alloy microchannel. *Precis Eng*. 2024;88:251-265.
68. Ding H, Chen S, Cheng K. Two dimensional vibration-assisted micro-milling: kinematics simulation , chip thickness computation and analysis. *Adv. Mater. Res* 2010;(97-101):2779-2784.
69. Yi J, Liu X, Wang T, et al. Surface quality study of longitudinal torsional ultrasonic micro-milling of borosilicate glass based on morphological modeling. *Int J Adv Manuf Technol* 2024;133(1-2):183-198.
70. Ibrahim R, Rafai NH, Rahim EA, et al. A study of tool motion in 2 dimensional ultrasonic assisted micro-milling. *Applied Mechanics & Materials*. 2015;815:328-331.
71. Chen W, Zheng L, Huo D, et al. Surface texture formation by non-resonant vibration assisted micro milling. *J Micromechanics Microengineering*. 2018;28(2):025006.
72. Zheng L, Xie W, Huo D. Modelling and experimental investigation on textured surface generation in vibration-assisted micro-milling. *J of Materials Process Technol*. 2019;266:339-350.
73. Zhang X, Yu T, Wang W. Dynamic cutting force prediction for micro end milling considering tool vibrations and run-out.*P I Mech Eng C-J Mec* 2019;233(7):2248-2261.
74. He J, Guo Z, Lian H, et al. Improving the machining quality of micro structures by using electrophoresis-assisted ultrasonic micromilling machining. *Int J Precis Eng Manuf - Green Technol*. 2020; 7(1): 151-161.
75. Sobamowo MG, Ojolo SJ, Olawale OK, et al. Force modeling and dynamic behaviour of multi-dimensional vibration assisted micro-end milling: Linear and nonlinear analyses. 2020;143(February):224-261.
76. Yuan Z, Fang B, Dong Y, et al. Study on surface texture and corrosion

resistance of ultrasonic vibration-assisted micromilling Inconel718. *Int J Adv Manuf Technol*. 2022;121(1-2):601-618.
77. Shang P, Yang Z, Zhang H, et al. Study on the mechanism of bone temperature diffusion in vibration-assisted micro milling. *2022 IEEE Int Conf Manip Manuf Meas Nanoscale*. 2022;(August):349-354.
78. Yuan Z, Fang B, Zhang Y, et al. Effect of cutting parameters on chips and burrs formation with traditional micromilling and ultrasonic vibration assisted micromilling. *Int J Adv Manuf Technol*. 2022; 119(3-4): 2615-2628.
79. Su ZP, Liang ZQ, Li J, et al. Experimental research on ultrasonic spiral assisted milling and grinding of titanium alloy micro groove. *Journal of Mechanical Engineering* 2024;60(09): 5-12.
80. Aramcharoen A, Mativenga PT. Size effect and tool geometry in micromilling of tool steel. *Precis Eng*. 2009;33(4):402-407.
81. Balázs BZ, Takács M. Experimental investigation and optimisation of the micro milling process of hardened hot-work tool steel. *Int J Adv Manuf Technol*. 2020;106(11-12):5289-5305.
82. Fang B, Yuan Z, Li D, et al. Effect of ultrasonic vibration on finished quality in ultrasonic vibration assisted micromilling of Inconel718. *Chinese J Aeronaut*. 2021;34(6):209-219.
83. Kim GD, Loh BG. Characteristics of chip formation in micro V-grooving using elliptical vibration cutting. *J Micromech Microeng*. 2007;17 (8): 1458-1466.
84. Li G, Li YH, Liao QY, et al. Mechanism of dual-direction vibration-assisted (DVA) micro-milling in surface formation considering the tool life-lengthening effect on the Ti6Al4V: design and experiment. *Int J Adv Manuf Technol*. 2022;123(7-8):2313-2330.
85. Chen W, Zheng L, Teng X, et al. Finite element simulation and experimental investigation on cutting mechanism in vibration-assisted micromilling. *Int J Adv Manuf Technol*. 2019;105(11):4539-4549.
86. Gillespie LK. The formation and properties of machining burrs. *Journal of Manufacturing Science & Engineering.* 1976.
87. Aurich JC, Dornfeld D, Arrazola PJ, et al. Burrs-analysis, control and removal. *CIRP Ann - Manuf Technol*. 2009;58(2):519-542.
88. Hashimura M, Hassamontr J, Dornfeld DA. Effect of in-plane exit angle and rake angles on burr height and thickness in face milling operation. *J Manuf Sci Eng Trans ASME*. 1999;121(1):13-19.
89. Carlos L, Rosa P. Study of burr behavior in face milling of PH 13-8 Mo stainless steel. *CIRP J Manuf Sci Tec*. 2015;1:1-9.
90. Piquard R, D'Acunto A, Laheurte P, et al. Micro-end milling of NiTi biomedical alloys , burr formation and phase. *Precis Eng* . 2014; 38: 356-364.
91. O’Toole L, Kang CW, Fang FZ. Precision micro-milling process: state of the art. *Adv Manuf*. 2021;9(2):173-205.
92. Kai Y, Ba IQ, Fu YU, et al. Modeling and experimental analysis of the mechanism of micro-burr formation in micro-end-milling process . *Nanotechnology and Precision Engineering*. 2010;8(1):75-83.
93. Wan Y, Cheng K, Sun S. An innovative method for surface defects prevention in micro milling and its implementation perspectives. *P I Mech Eng J-J Eng*. 2013;227(12):1347-1355.
94. Xing Q, Gao M, Yao Z, et al. Research on ultrasonic vibration-assisted micro-EDM milling of microgrooves with large aspect ratio. *Int J Adv Manuf Technol*. 2023;128(3-4):1629-1639.
95. Li G, Wang B, Xue J, et al. Development of vibration-assisted micromilling device and effect of vibration parameters on surface quality and exit-burr. *P I Mech Eng B-J Eng*.2019;233(6):1723-1729.
96. Han G, Pan G, Wu W, et al. Research on the burr forming characteristics of ultrasonic assisted micro-milling process. *Trans Beijing Inst Technol*. 2018;38(9).
97. Ciftci I, Turker M, Seker U. Evaluation of tool wear when machining SiCp-reinforced Al-2014 alloy matrix composites. *Mater Des*. 2004;25 (3):251-255.
98. Zhu D, Zhang X, Ding H. Tool wear characteristics in machining of nickel-based superalloys. *Int J Mach Tools Manuf*. 2013;64:60-77.
99. Kuntoğlu M, Sağlam H. Investigation of progressive tool wear for determining of optimized machining parameters in turning. *Meas J Int Meas Confed*. 2019;140:427-436.
100. Lan TS, Chuang KC, Chen YM. Optimization of machining parameters using fuzzy Taguchi method for reducing tool wear. *Appl Sci*. 2018;8(7).
101. Oliaei SNB, Karpat Y. Influence of tool wear on machining forces and tool deflections during micro milling. *Int J Adv Manuf Technol*. 2016; 84(9-12):1963-1980.
102. Lv D. Influences of high-frequency vibration on tool wear in rotary ultrasonic machining of glass BK7. *Int J Adv Manuf Technol*. 2016;84(5-8):1443-1455.
103. Liu Y, Liu Z, Wang X, et al. Experimental study on tool wear in ultrasonic vibration-assisted milling of C/SiC composites. *Int J Adv Manuf Technol*. 2020;107(1-2):425-436.
104. Ding H, Ibrahim R, Cheng K, et al. Experimental study on machinability improvement of hardened tool steel using two dimensional vibration-assisted micro-end-milling. *Int J Mach Tools Manuf*. 2010;50(12): 1115-1118.
105. Budinski KG. Tool wear in cutting plastic - abrasion or erosion? *Wear*. 1999;233-235:362-371.
106. Wang Z, Kovvuri V, Araujo A, et al. Built-up-edge effects on surface deterioration in micromilling processes. *J Manuf Process*. 2016; 24: 321-327.
107. Davoudinejad A, Tosello G, Annoni M. Influence of the worn tool affected by built-up edge (BUE) on micro end-milling process performance: A 3D finite element modeling investigation. *Int J Precis Eng Manuf*. 2017;18(10):1321-1332.
108. Yuan Z, Dong Y, Ding H, et al. Study on surface quality and corrosion resistance of ultrasonic vibration assisted micromilling Inconel718. *Int J Adv Manuf Technol*. 2022;121(1-2):601-618.
109. Ibrahim MR, Rahim Z, Rahim E, et al. An Experimental investigation of cutting temperature and tool wear in 2 dimensional ultrasonic vibrations assisted micro-milling. *MATEC Web Conf*. 2017;95:07005.
110. Chen W, Teng X, Huo D, et al. An improved cutting force model for micro milling considering machining dynamics. *Int J Adv Manuf Technol*. 2017;93(9-12):3005-3016.
111. LIU X, WANG W, JIANG R, et al. Analytical model of cutting force in axial ultrasonic vibration-assisted milling in-situ TiB2/7050Al PRMMCs. *Chinese J Aeronaut*. 2021;34(4):160-173.
112. Verma GC, Pandey PM, Dixit US. Modeling of static machining force in axial ultrasonic-vibration assisted milling considering acoustic softening. *Int J Mech Sci*. 2018;136(December 2017):1-16.
113. Shen X, Zhang J, Yin T, et al. A study on cutting force in micro end milling with ultrasonic vibration. *Adv Mater Res*. 2010;97-101:1910-1914.
114. Kim GD, Loh BG. Machining of micro-channels and pyramid patterns using elliptical vibration cutting. *Int J Adv Manuf Technol*. 2010;49(9-12): 961-968.
115. Xu L, Liu Z, Han G, et al. Experimental study on ultrasonic assistant micro-milling of 45# steel under different grain size conditions. *Trans Beijing Inst Technol*. 2018;38(11):1105-1110.
116. Xu L, Chen Y, Han G, et al. Machinability research on the ultrasonic assisted micro-milling for graphene based aluminum matrix composite. *Trans Beijing Inst Technol*. 2022;41(8):894-900.
117. Hu H, Sun Y, Lu Z. Simulation and experiment of cutting force in ultrasonic torsional vibration assisted micro-milling. *5th Int Symp Adv Opt Manuf Test Technol Des Manuf Test Micro- Nano-Optical Devices Syst*.
118. Parenti P, Park CI, Park SS, et al. Increasing stability of meso / micro milling cutting by means of ultrasonic vibration assisted machining piezo-electric actuators. Published online 2014:8536.
119. Shang P, Liu X, Zhang H, et al. Research on cutting force of vibration-assisted micro-milling of bone materials. *2022 IEEE Int Conf Manip Manuf Meas Nanoscale, 3M-NANO 2022 - Proc*. 2022.p.344-348.
120. Prabhu P. Investigations on piezo actuator-based nonresonant type workpiece vibratory system for vibration- assisted micro-milling. *J Micromechanics Microengineering*. 2023;35(8):657-672.

121. Wissmiller DL, Pfefferkorn FE. Technical paper: Micro end mill tool temperature measurement and prediction. *J Manuf Process*. 2009; 11 (1):45-53.
122. Mamedov A, Lazoglu I. Thermal analysis of micro milling titanium alloy Ti-6Al-4V. *J Mater Process Technol*. 2016;229(October 2015):659-667.
123. Yang K, Liang YC, Zheng KN, et al. Tool edge radius effect on cutting temperature in micro-end-milling process. *Int J Adv Manuf Technol*. 2011;52(9-12):905-912.
124. Elsadek AA, Gaafer AM, Mohamed SS, et al. Prediction and optimization of cutting temperature on hard-turning of AISI H13 hot work steel. *SN Appl Sci*. 2020;2(4):1-12.
125. Sun YJ, Gong H, Gui SY, et al. Towards understanding the cutting temperature in ultrasonic vibration-assisted drilling based on the dynamic contact characteristics between the cutting edge and workpiece. *Ultrasonics*. 2023;135(August):107131.
126. Liu X, Wang W, Jiang R, et al. Analytical model of workpiece temperature in axial ultrasonic vibration-assisted milling in situ TiB2/7050Al MMCs. *Int J Adv Manuf Technol*. 2022;119(3-4):1659-1672.
127. Chen L, Deng D, Pi G, et al. Burr formation and surface roughness characteristics in micro-milling of microchannels. *Int J Adv Manuf Technol*. 2020;111(5-6):1277-1290.
128. Biermann D, Steiner M. Analysis of micro burr formation in austenitic stainless steel X5CrNi18-10. *Procedia CIRP*. 2012;3(1):97-102.
129. Uhlmann E, Piltz S, Schauer K. Micro milling of sintered tungsten-copper composite materials. *J Mater Process Technol*. 2005;167(2-3): 402-407.
130. Serje D, Pacheco J, Diez E. Micromilling research: current trends and future prospects. *Int J Adv Manuf Technol*. 2020;111:1889-1916.
131. Li KM, Chou SY. Journal of materials processing technology experimental evaluation of minimum quantity lubrication in near micro-milling. *J Mater Process Tech*. 2010;210(15):2163-2170.
132. Shaw C. Energy conversion in cutting and grinding. *CIRP Ann*. 1996; 45(1):101-104.
133. Search H, Journals C, Contact A, et al. An investigation of cutting mechanics in 2 dimensional ultrasonic vibration assisted milling toward chip thickness and chip formation. *3rd International Conference of Mechanical Engineering Research*. 2015;100:012057.
134. Liu X, Wang W, Jiang R, et al. Investigation on surface roughness in axial ultrasonic vibration-assisted milling of in situ TiB2/7050Al MMCs. *Int J Adv Manuf Technol*. 2020;111(1-2):63-75.
135. Kiswanto G, Johan YR, Ko TJ. Machined surface roughness geometry model development on ultrasonic vibration assisted micromilling with end mill. *Key Engineering Materials* 2020;846(1):122-127.
136. Guo L, Fei D, Bo W, et al. Study on the micro-milling of optical microstructure with the assist of the workpiece vibration. *7th international Symposium on Advanced Optical Manufacturing and Testing Technologies: Design, Manufacturing, and Testing of Micro- and Nano-optical Devices and Systems.* 2014;9283:1-6.
137. Jin X, Xie B. Experimental study on surface generation in vibration-assisted micro-milling of glass. *Int J Adv Manuf Technol.* 2015;81(1-4):507-512.
138. Du Y, Song Q, Liu Z. Prediction of micro milling force and surface roughness considering size - dependent vibration of micro - end mill. *Int J Adv Manuf Technol*. 2022;119(9-10):5807-5820.
139. Hu HJ, Sun YZ, Lu ZS. Simulation of residual stress in ultrasonic vibration assisted micro-milling. *Adv Mater Res*. 2011;188:381-384.
140. Chen W, Huo D, Hale J, et al. Kinematics and tool-workpiece separation analysis of vibration assisted milling. *Int J Mech Sci*. 2018;136(July 2017):169-178.
141. Lu Z, Hu H, Sun, Y, et al. Study on residual stresses in Ultrasonic Torsional Vibration Assisted Micro-milling. *5th International Symposium on Advanced Optical Manufacturing and Testing Technologies: Design, Manufacturing, and Testing of Micro- and Nano-optical Devices and Systems*. 2010;7657:1-5.
142. Fritz K. *Manufacturing processes*. Springer Berlin Heidelberg. 2011
143. Milton CS, Cookson JO. Metal cutting principles. *Tribology International*. 1989;18(1):55.
144. Kim JS, Kim JW, Lee SW. Experimental characterization on micro-end milling of titanium alloy using nanofluid minimum quantity lubrication with chilly gas. *Int J Adv Manuf Technol.* 2017;91(5-8): 2741-2749.
145. Sun J, Wong YS, Rahman M, et al. Effects of coolant supply methods and cutting conditions on tool life in end milling titanium alloy. *Mach Sci Technol*. 2006;10(3):355-370.
146. Rahman M, Wang ZG, Wong YS. A Review on ultrasonic machining of titanium alloys. *JSME Int Journal, Ser C Mech Syst Mach Elem Manuf*. 2006;49(1):11-20.
147. Kumar Wagri N, Petare A, Agrawal A, et al. An overview of the machinability of alloy steel. *Mater Today Proc*. 2022;62:3771-3781.
148. Hafiz MSA, Kawaz MHA, Mohamad WNF, et al. A review on feasibility study of ultrasonic assisted machining on aircraft component manufacturing. *IOP Conf Ser Mater Sci Eng*. 2017;270(1).
149. Santos MC, Machado AR, Sales WF, Barrozo MAS, Ezugwu EO. Machining of aluminum alloys: a review. *Int J Adv Manuf Technol*. 2016; 86(9-12):3067-3080.
150. Dandekar CR, Shin YC. Modeling of machining of composite materials: A review. *Int J Mach Tools Manuf*. 2012;57:102-121.
151. Toulfatzis AI, Pantazopoulos GA, David CN, et al. Machinability of eco-friendly lead-free brass alloys: Cutting-force and surface-roughness optimization. *Metals (Basel)*. 2018;8(4):1-18.
152. Kumar NS, Harsha P, Sudharshan N, et al. A Review on machining process of glass materials. *Int J Res Eng Sci Manag*. 2016;15(1): 17-19.